Geomorphology 430 (2023) 108650

Contents lists available at ScienceDirect

Geomorphology

journal homepage: www.journals.elsevier.com/geomorphology

What drives major channel widening in mountain rivers during floods? The role of debris floods during a high-magnitude event

A. Brenna [a,*], L. Marchi [b], M. Borga [c], M. Zaramella [c], N. Surian [a]

[a] Department of Geosciences, University of Padova, Padova, Italy
[b] Research Institute for Geo-hydrological Protection, National Research Council (CNR IRPI), Padova, Italy
[c] Department of Land, Environment, Agriculture and Forestry, University of Padova, Legnaro, Italy

ARTICLE INFO

Keywords:
Sediment transport
Debris flood
Geomorphological hazard
Cordevole river basin
Vaia storm

ABSTRACT

Our capability to accurately predict at the local scale the morphological changes in a mountain river affected by a severe flood is currently limited. Given the importance of including geomorphological hazards in flood risk evaluation, some improvements in this direction are required. In fact, on the basis of the controlling factors typically considered in the literature, that are the unit stream power (ω_{pk}) and the confinement index (CI), a relatively broad spectrum of width ratios (WR = ratio between channel width after a flood and channel width before a flood) occurring in response to major floods is commonly observed in streams. We extended previous research focused on parameters that influence the morphological response of a channel to a severe flood by investigating the role played by the type of sediment transport process that occurs in a mountain river. In particular, we explored whether a relationship exists between debris flood (i.e. a condition characterised by extremely high bedload) and intense channel widening. The case study was the Cordevole River (the Dolomites, Italy) and four of its tributaries, which were affected by the severe flooding induced by the Vaia storm in October 2018. WR was determined at the sub-reach scale, and ω_{pk} was calculated with consideration for the flood peak discharge ascertained via hydrological modeling. Despite the significant relationships found among WR, ω_{pk} and CI, 21 sub-reaches (out of 144) of the studied stream network widened intensely reaching a WR higher than approximately 4, often to a substantially larger extent than predicted by statistical models. Such sub-reaches were certainly or probably affected by debris floods, leading us to infer that debris floods can induce widening processes that are more intense than those occurring in response to water flows. Having said that, debris floods do not automatically imply very intense widening. In addition to hydraulic and morphological constraints, the sediment transport processes possibly taking place at a sub-reach of a mountain river should be regarded as another driver of channel modifications during high-magnitude hydrological events.

1. Introduction

The responses of rivers to floods have been a topic of considerable interest for the geomorphological community over the last decades (e.g. Baker et al., 1988; Baker, 1994). Some researchers have compared the roles played by high-magnitude hydrological events with those of frequent low-magnitude floods (e.g. Wolman and Miller, 1960; Gupta and Fox, 1974; Phillips, 2002), recognising the contribution of large to extreme events to determining the geomorphic evolution of a fluvial system for several river types and physiographic contexts (e.g. Kale and Hire, 2004; Hooke, 2015). The role played by severe flooding becomes crucial in mountain and coarse-bedded rivers (e.g. Lenzi et al., 2006a, 2006b; Molnar et al., 2010; Surian et al., 2016; Scorpio et al., 2018; Scorpio et al., 2022), intermittent rivers (e.g. Harvey, 1984; Hooke and Mant, 2000) and bedrock or semi-alluvial channels (e.g. Baker and Kale, 1998; Jansen, 2006; Righini et al., 2017). Several researchers have therefore focused on the channel modifications induced by such events, documenting how river morphologies change in response to large floods (e.g. Hauer and Habersack, 2009; Krapesch et al., 2011; Belletti et al., 2014; Scorpio et al., 2018). These changes include widening, island erosion and development, floodplain accretion and alterations to bed elevation, channel position and channel pattern.

Increasing attention has also been devoted to the analyses of controlling factors for the geomorphic effectiveness of the high-magnitude

* Corresponding author at: Via G. Gradenigo, 6, 35131 Padova, Italy.
E-mail address: andrea.brenna@unipd.it (A. Brenna).

https://doi.org/10.1016/j.geomorph.2023.108650
Received 24 June 2022; Received in revised form 1 January 2023; Accepted 6 March 2023
Available online 16 March 2023

events. Such examinations initially identified hydraulic variables, such as flow competence, stream power, unit stream power and the flow duration above a critical threshold, as significant parameters for determining channel responses to large floods (Magilligan, 1992; Costa and O'Connor, 1995; Magilligan et al., 1998; Cenderelli and Wohl, 2003; Kale, 2007; Magilligan et al., 2015). However, Langhammer (2010), Krapesch et al. (2011), Dean and Schmidt (2013), Thompson and Croke (2013) and Buraas et al. (2014) asserted that hydraulic variables alone cannot fully explain a river's morphological response to hydrological events, with the authors stressing the importance of considering the presence of human structures, bedload supply, pre-flood channel arrangement and lateral confinement to accurately predict a channel's response to a large flood. Applying Rinaldi et al.'s (2016) integrated approach to investigating the geomorphic responses of rivers to extreme events, Surian et al. (2016) demonstrated the need of simultaneously inquiring into several controlling factors. Surian et al. (2016) concluded that the unit stream power calculated on the basis of the pre-flood width of a channel and its lateral confinement are the most significant factors for explaining the degree of channel widening that occurred in six mountain rivers of the Apennines (Italy) during a major flood in October 2011. These authors also found weaker relationships of channel widening with the percentage of river reach length protected by artificial structures and the sediment supply area.

The aforementioned research efforts have improved our understanding of the responses of fluvial systems to high-magnitude floods, but our capability to accurately predict the morphological changes in a stream affected by a severe flood, especially at the local scale, remains limited, as evidenced by the metrics of regression models that relate channel widening to controlling hydraulic and morphological factors (Surian et al., 2016; Scorpio et al., 2018). The combination of unit stream power and the confinement index may produce a relatively broad spectrum of channel responses (e.g. different width ratios, calculated as the widths before and after a flood). Because of the importance of including geomorphological hazards in flood risk evaluation (e.g. Krapesch et al., 2011; Rinaldi et al., 2015; Braud et al., 2016), some improvements in this direction are required.

Rinaldi et al. (2016) identified hydrological and hydraulic variables, sediment sources, channel changes, degree of human interventions and sediment transport processes as crucial factors that should be taken into account in studying the response of a channel to a severe flood. Among these factors, the recognition of sediment transport processes occurring along a stream during a high-magnitude floods is currently a minimally considered issue in geomorphic literature. Sediment transfer in mountain rivers occurs via a range of sediment transport processes, often referred in literature as "sediment–water flow types" (e.g. Pierson et al., 1987), classified as *water flows, debris flows*, *hyperconcentrated flows* and *debris floods* (Church and Jakob, 2020; Brenna et al., 2020a). *Water flow* is a fluid gravity flow that refers to the transport of particles mobilized by the competence of flowing water acting on each individual grain (Waananen et al., 1970; Kuhnle, 2013; Yager and Schott, 2013; Hicks and Gomez, 2016). It includes the movement of particles in suspension within the water column (suspended load) and in contact with the streambed (bedload). The concentration of suspended sediment is <4 % by volume with the fluid typified by liquid behaviour and turbulent flow. Bedload can range from a partial entrainment of the finer particles overpassing a static bed (bedload stage 1, according to Carling, 1988) to the entire mobilization of the streambed material (stage 3). *Debris flow* is a sediment gravity flow occurring as a mass movement (Costa, 1984, 1988; Iverson, 1997, 2003) definable as the 'gravitational movement of a shearing, highly-concentrated, yet relative mobile, mixture of debris and water' (Blikra and Nemec, 1998). Debris flows comprise a sediment concentration that may exceed 60 % in volume, which thereby determines their flow rheology definable as non-Newtonian. *Hyperconcentrated flows* are fluid gravity flows highly charged with fine and/or low-density particles mobilized in suspension (from 20 % to 60 % by volume), definable in rheological terms as variably turbulent, plastic and non Bingham flows with an apparent liquid behaviour (Beverage and Culbertson, 1964; Pierson et al., 1987; Costa, 1988; Rickenmann, 1991; Coussot and Meunier, 1996; Nemec, 2009). They occur mainly in volcanoclastic and arid alluvial settings (e.g. Mather and Hartley, 2005; Pierson and Major, 2014). *Debris floods* are 'water-driven flood flows with high bedload transport' (Church and Jakob, 2020), during which a 'streambed may be destabilised causing massive movement of sediment' (Hungr et al., 2014) with the establishment of a slurry-like flow of entrained sediment characterised as an incipient granular mass flow (Manville and White, 2003), representing a severe case of stage 3 (sensu Carling, 1988) bedload transport. Debris floods are a common phenomenon in high-gradient channels with abundant coarse sediment (e.g. mountain rivers), and their occurrence is promoted during severe floods in response to high hydrological forcing (e.g. high water discharge in steep and narrow channels) or downstream of tributaries that deliver large amounts of sediment to a receiving stream via debris flows (Brenna et al., 2021). Church and Jakob (2020) and Jakob et al. (2022) stated that extraordinary widening often characterises channel sites affected by a debris flood because of extensive bank erosion. Consistent with this assertion, the preliminary results obtained by Brenna et al. (2021), who looked into channel changes in a stream in the Dolomites (Italy) after a severe flood, suggest that at the same unit stream power, channel sites affected by debris floods experience channel widening that is two to three times larger than the widening in sites where ordinary water flows occur.

In consideration of the discussion above, the research questions pursued in this work are as follows: (1) Is the typology of fluid gravity flow occurring at a channel site one of the main drivers of channel responses to high-magnitude floods? More specifically, (2) is there a relationship between debris floods and intense channel widening? To illuminate these issues, we explored five mountain rivers in the Eastern Italian Alps, where various sediment–water flow types can occur during severe hydrological events. We particularly focused on channel widening, being a dominant geomorphological process in mountain rivers during large floods and being relatively easier to measure compared with other channel responses (e.g. bed elevation changes). The aim of this research was to shed light on the roles played by water flows versus debris floods in the determination of channel widening during high-magnitude floods in mountain rivers.

We expect that improving our capability to predict the morphological responses of mountain streams to severe hydrological events will lead to more accurate assessment of geomorphological hazards at the local scale. A reliable prediction of geomorphic hazards represents a crucial requirement for achieving an accurate definition of the risk induced by floods in mountain rivers (Krapesch et al., 2011; Rinaldi et al., 2015; Braud et al., 2016). A case in point is Ruiz-Villanueva et al. (2018), who recently underscored the "need to continue documenting and analysing channel widening after floods […] for a better process understanding" because "the identification of controlling factors can contribute to the identification of critical reaches, which in turn is crucial for the forecasting and design of sound river basin management strategies".

The case study selected to answer the research questions is the Cordevole river basin (the Dolomites, Italy), which was affected in October 2018 by a severe rainstorm named "Vaia". Apart from examining the main stem of the Cordevole River, we considered three of its tributaries (Pettorina, Liera and Corpassa torrents), which were affected to different intensities by the flooding induced by Vaia and which are characterised by a range of human interventions (e.g. bank protections) and morphological and sedimentological channel features. To these sites of interest, we added the Tegnas Torrent, which was analysed in detail by Brenna et al. (2020a, 2020b, 2021) and Pellegrini et al. (2021). Debris flows were disregarded from the quantitative analysis of channel widening because they are sediment gravity flows with peculiar rheological features and dynamics, which preclude their direct comparison with fluid gravity flows (i.e. water flows and debris floods). Moreover, although debris flows are common in steep, small tributaries, they do not occur in this work's channel of interest, or their occurrence is restricted to a few headwater channel reaches. Hyperconcentrated flows were also excluded from the investigation because the majority of mountain catchments in alpine environments primarily produce coarse debris (e.g. Sklar et al., 2020), and the dominant transport process under paroxysmal conditions is debris flooding (Brenna et al., 2021).

2. General setting

2.1. Study area

The Cordevole river basin is located in the Dolomites (Eastern Italian Alps), covering an area of 857 km^2 with an elevation ranging from 280 to 3343 m a.s.l. and exhibiting elongation in the NNW–SSE direction (Fig. 1). The catchment is composed mainly of dolostone, limestone, volcanic rocks and Quaternary deposits. Woodlands cover approximately 40 % of the territory (Rigon et al., 2013). The climate is typically alpine with cold and snowy winters and temperate summers. The mean annual precipitation is approximately 1100 mm, with most of the intense precipitation occurring in autumn and during summer storms (Rigon et al., 2013).

The mean water discharge of the Cordevole River at Ponte Mas gauging station (705 km^2) is 7.7 m^{3}s^{-1} (ARPAV, 2019), and its hydrological regime is characterised by higher discharge during the snowmelt period (May–June), frequent floods during autumn and summer and lower flow conditions during the coldest months (December–February). Along the Cordevole River and its tributaries, check dams, bank protections and artificial levees are widespread. A small reservoir for power production is found in the Cencenighe Agordino village (Ghirlo reservoir), and a natural lake (Alleghe Lake) is regulated for power production (Fig. 1). Other reservoirs within the Cordevole river basin are located in the Biois catchment (Cavia Lake) and on the Mis Torrent (Mis Lake).

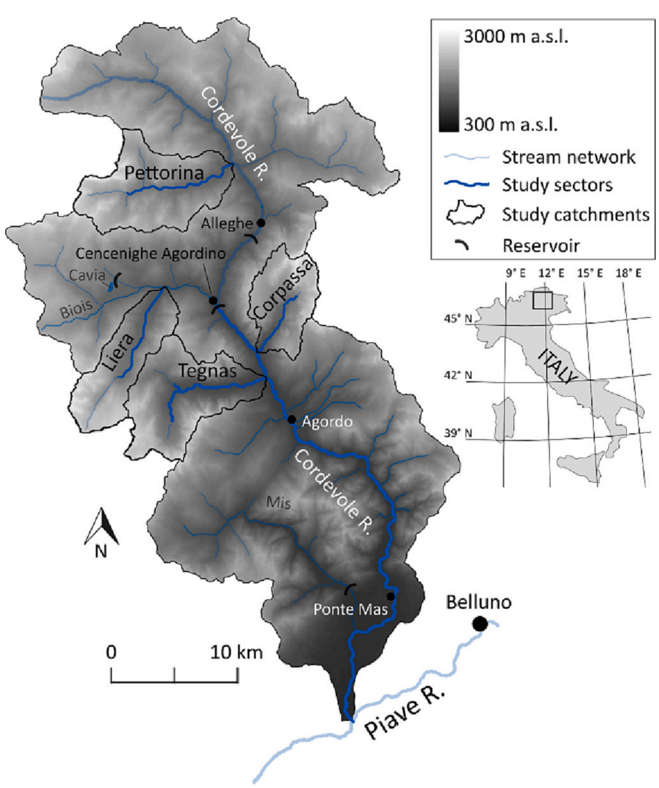

Fig. 1. Location map of the Cordevole river basin, the tributaries in the studied catchments and the studied sectors.

Our work focused on a sector of the Cordevole River with a length of 41 km downstream from Cencenighe Agordino to its confluence with the Piave River (Fig. 1). We also considered a left tributary (Corpassa Torrent) and two right tributaries (Pettorina and Tegnas torrents) of the Cordevole River and the Liera Torrent that is a tributary of the Biois Torrent, which in turn flows into the Cordevole River near Cencenighe Agordino (Fig. 1). These five streams were selected because they display different morphological characteristics (e.g. an average channel width before flooding that ranges from 5 to 80 m in the Liera Torrent and Cordevole River) and occurrence of human structures (e.g. very low in the Corpassa Torrent whereas high in the Pettorina Torrent; see Supplementary Material). The main characteristics of the investigated streams are presented in Table 1.

2.2. The Vaia storm

The Vaia storm, accompanied with intense and prolonged rainfall with recurrence time of precipitation exceeding 200 years in the mountainous area associated with exceptional wind storms, led to casualties and heavy damage in northeastern Italy, particularly in the studied basins (Motta et al., 2018; Cavaleri et al., 2019; Davolio et al., 2020; Forzieri et al., 2020; Giovannini et al., 2021). The precipitation event occurred in two phases: the first was characterised by the orographic enhancement of precipitation, lasting for two days (27–28 October 2018), and the second, which developed from October 29 to 30, was characterised by intense convective precipitation over saturated soils. Fig. 2a shows the cumulative rainfall during the entire event over the whole Cordevole river basin, reflecting remarkable precipitation gradients, with the highest cumulative rainfall (up to 716 mm) occurring in the central region of the basin. Fig. 2b indicates the cumulative precipitation over the period 17:00 to 20:00 CET, 29 October 2018, during which a convective band controlled the formation of peak discharges, debris flows and debris floods.

3. Materials and methods

3.1. River network segmentation and morphological characteristics before the flood

All the analyses conducted in this work were carried out at the spatial scale of a channel sub-reach. First, the studied channels (which add to a total length of 73.5 km) were partitioned into homogeneous reaches using the methodology proposed by Brierley and Fryirs (2005) and Rinaldi et al. (2013), which takes into account the occurrence of discontinuities (e.g. the confluence of tributaries) and relevant changes in

Table 1
Characteristics of the analysed streams and the number of reaches and sub-reaches considered in the study. The average slope of the analysed channel length and maximum and minimum slopes determined at the sub-reach scale (in brackets) are also reported. Drainage areas were determined from a 30 m resolution DEM (https://asterweb.jpl.nasa.gov/gdem.asp) used for hydrological modeling.

River	Drainage area (km^2)	Analysed channel length (km)	Average channel slope (%)	Number of reaches	Number of sub-reaches
Cordevole	856.9	41.0	1.14 [3.46–0.10]	14	53
Corpassa	25.3	4.5	12.05 [18.17–8.25]	3	15
Pettorina	53.9	9.3	6.07 [16.39–0.91]	5	27
Tegnas	51.4	9.9	5.51 [7.35–1.99]	7	27
Liera	39.9	8.8	4.98 [21.27–0.28]	6	22

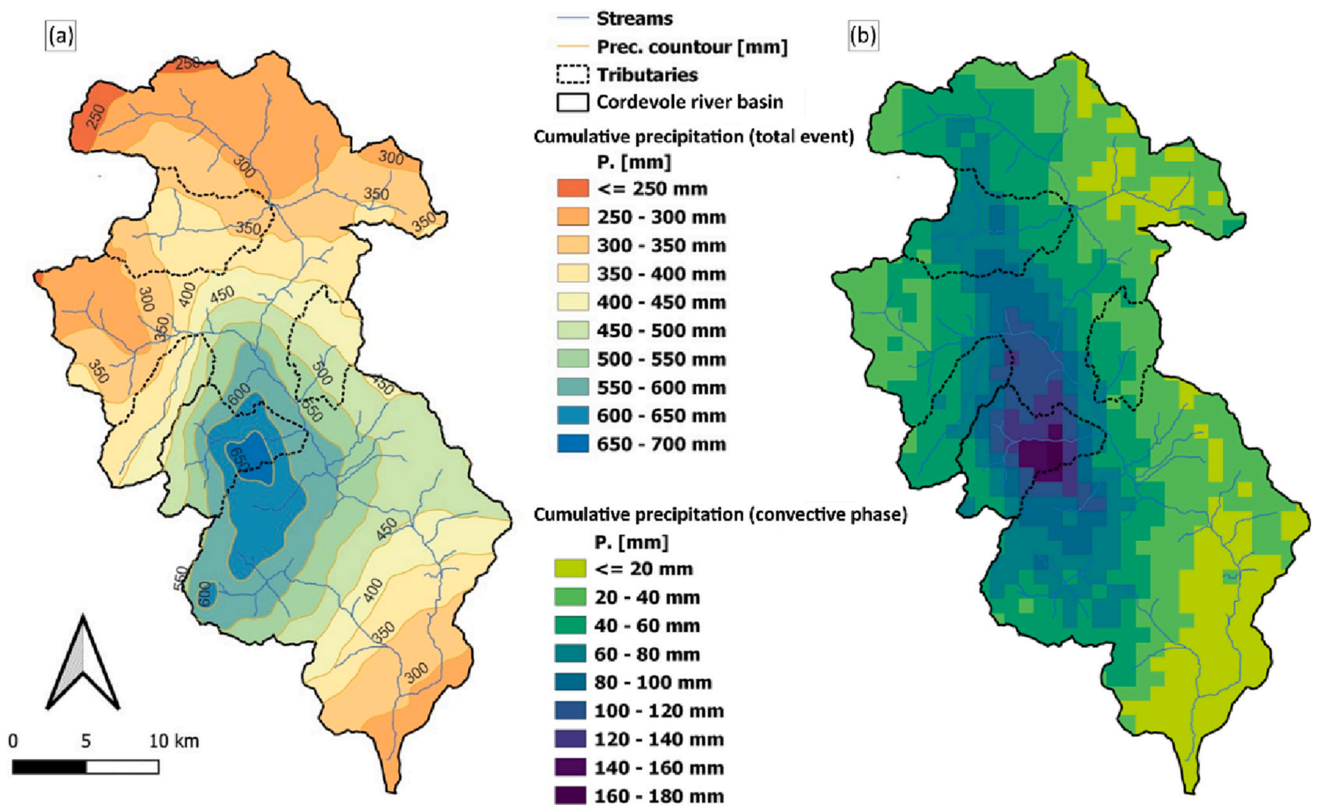

Fig. 2. Cumulative precipitation over the Cordevole river basin (a) during the entire event and (b) during the convective phase (17:00–20:00 CET, 29 October 2018).

channel lateral confinement, width, slope and morphological pattern. Then, as in Surian et al. (2016), Righini et al. (2017) and Scorpio et al. (2018), the GIS-based procedure developed by Ferencevic and Ashmore (2012) was applied to divide each reach into sub-reaches with lengths equal to the proper minimum distance required to extract a DEM-derived (digital elevation model) slope of satisfactory quality for the stream power calculation (see Section 3.3). The segmentation was carried out by employing a DEM with a 5 m resolution derived from 1:5000-scale topographic map (Carta Tecnica Regionale, CTR) that has a vertical accuracy typically around ±0.5 m and 0.2 m resolution aerial photographs acquired by the Veneto Region in 2015 (http://idt2.regione.veneto.it). We defined 117 sub-reaches (Table 1) with lengths ranging from a minimum of 180 m in the Corpassa Torrent to a maximum of 940 m in the Cordevole River. We also covered the 27 sub-reaches determined by Brenna et al. (2020a) along the Tegnas Torrent and the terminal sector of its main tributary (Bordina Torrent) in the analyses (Table 1).

Following the criteria and methodologies adopted by Surian et al. (2016), the DEM, CTR and the aerial photographs were used to evaluate a number of parameters characterising each sub-reach before the Vaia event. The 2015 aerial photographs were considered representative of the channels at the time of the Vaia flood, as remarkable hydrological events did not occur between 2015 and October 2018. The 2015 channels, islands and floodplains were manually digitized in ArcGIS 10.5 (Fig. 3a and c). The mean channel width (referring to the active channel, which includes low-flow channels and unvegetated or poorly vegetated bars; islands were excluded) of each sub-reach before the Vaia event (W_{pre}) was determined as the ratio between an active channel area and its length; the slope of the sub-reach channel (S) was derived from the DEM. Similarly, the average width of the floodplain before the flood (F_{pre}) was calculated at the sub-reach scale. The sub-reach confinement index (CI) was ascertained from the ratio between F_{pre} and W_{pre} (Rinaldi et al., 2013). Moreover, the percentage of sub-reach length where the lateral mobility of the channel is potentially limited by the presence of longitudinal artificial structures (AS) was evaluated by identifying the artificial levees and bank protections visible from the aerial photographs or reported in the CTR.

3.2. *Analysis of channel widening*

To evaluate the morphological changes induced by Vaia in the examined rivers, the channels, islands and floodplain margins were re-digitized from two sets of images acquired after the Vaia flood (Fig. 3b and d). Specifically, the 0.2 m resolution aerial photographs acquired by the Veneto Region between June and September 2019 (Fig. 3d) were used to look into the tributaries and the Cordevole River at a sector located between Cencenighe Agordino and Agordo (Fig. 1). A SPOT 6 satellite image with a resolution of 1.5 m (Fig. 3b) and acquired in November 2018 was employed in the analysis of a site in the Cordevole River located between Agordo and its confluence with the Piave River (Fig. 1) given that aerial photographs of this river sector were unavailable.

The mean channel width of each sub-reach after the Vaia event (W_{post}) and the average width of the floodplain after the flood (F_{post}) were determined using polygons digitized from post-event images. The Vaia-induced channel widening was assessed on the basis of the width ratio (WR), calculated as the ratio between W_{post} and W_{pre} (Krapesch et al., 2011) for the 117 sub-reaches defined in this work. WR data were already available for the 27 sub-reaches of the Tegnas Torrent (Brenna et al., 2021). The GIS analysis can introduce a spectrum of errors (e.g. Mount et al., 2003), especially on the assessment of bank erosion and the temporal migration of channel axis that are significantly impacted by the co-registration of images. In this work, we were interested in evaluating the relative changes of channel width in terms of WR. For this reason, we restricted our analysis to errors affecting the channel width measure that are related to image interpretation and digitization. The error was calculated using a module of the approach of Swanson et al. (2011) as $2^{1/2}pR$, where R is the image resolution and p is the mean of

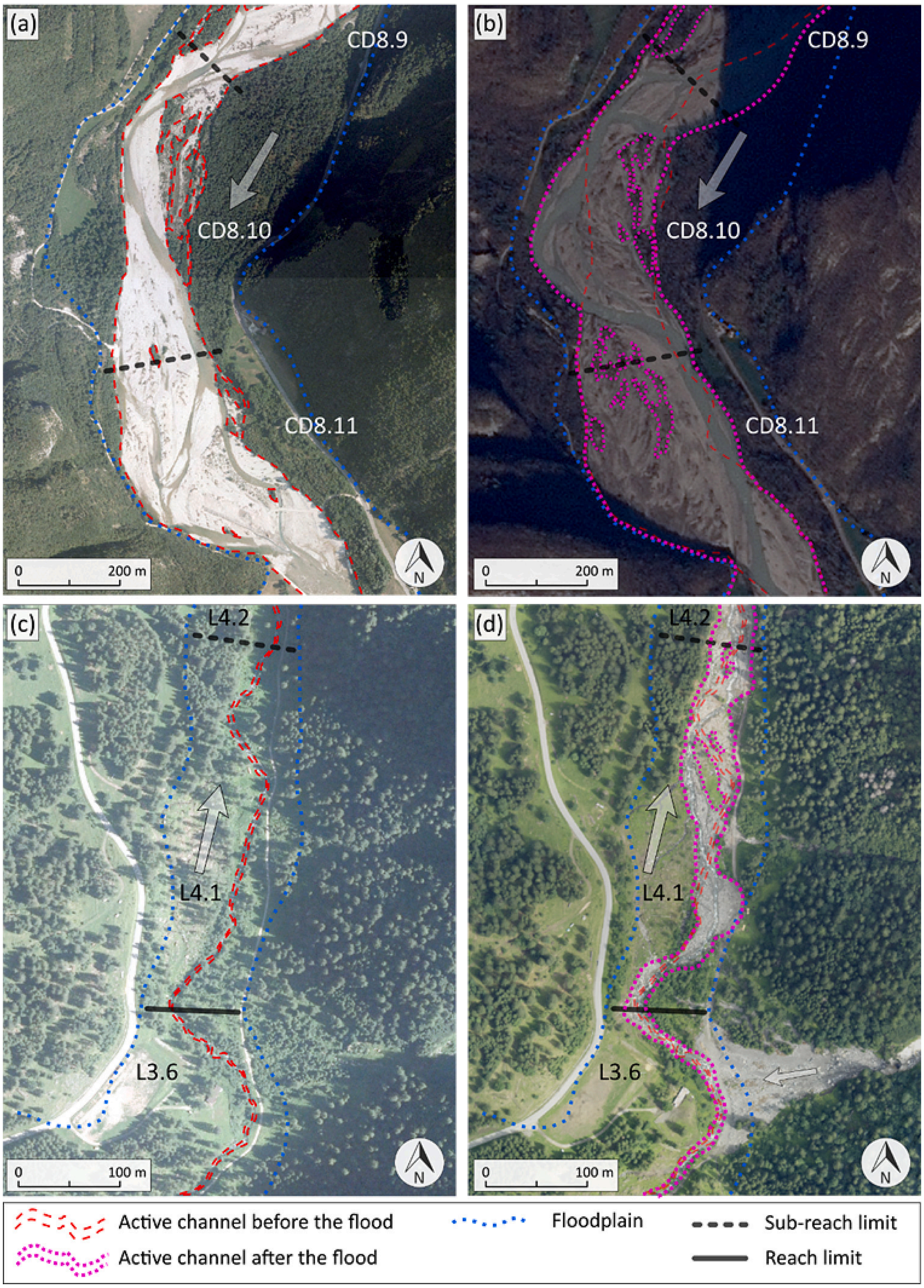

Fig. 3. Pre-flood (a, c) and post-flood (b, d) aerial photographs (a, c, d; 0.2 m resolution) and satellite images (b; 1.5 m resolution) showing the morphological changes induced by the Vaia event along two studied sectors of the Cordevole River (a, b; sub-reaches CD8.9, CD8.10 and CD8.11) and the Liera Torrent (c, d; sub-reaches L3.6, L4.1 and L4.2). Panel (d) shows a right tributary that was affected by debris flow during the Vaia event and delivered a large amount of sediments to the Liera main stem at sub-reach L3.6. The white arrows indicate flow direction.

the maximum number of pixels between two repeated digitisations of channel banks at a site of the stream network. These delineations were exploratorily conducted at ten sites located in the Pettorina and Liera torrents, where, with R of 0.2 m and average p of 4 m, it was reasonable to account for an error of about ±1 m, which is mainly due to the presence of vegetation locally covering the channel banks. As observed by Surian et al. (2016), this error affecting channel width and, consequently, the WR estimations is rather small relative to the magnitude of width changes (see Section 4.1) and can be reasonably disregarded from the following analysis that mainly focuses on sub-reaches characterised by major channel changes.

3.3. Hydrological analysis

Precipitation analysis was based on data from a network of 20 rain gauges in the study area and rainfall estimates from two C-band weather radars covering the region. Weather radar data were corrected for a number of error sources, including beam blocking, attenuation and wind drift, and were merged with rain gauge-based rainfall estimations on the ground (Zaramella et al., 2020, 2023). The precipitation estimates were aggregated at 20 min temporal resolution and 100 m spatial resolution to provide input to the hydrological model. Stream gauge data and flood hydrographs at three stations managed by the Environmental Agency of the Veneto Region and those pertaining to three hydropower production reservoirs (Cavia, Ghirlo and Mis) are available. The stream gauge of Ponte Mas, which drains most of the catchment area (Fig. 1), recorded only part of the rising limb of the hydrograph because it was damaged during the flood just before the peak time.

Flood peak discharges for seven basins, including the reaches explored in this work, were reconstructed through post-flood surveys by using methods reported by Borga et al. (2019) and Amponsah et al. (2018). For the Pettorina river basin, peak discharge was reconstructed by surveying channel cross-sections and the energy slope of a straight channel reach, as well as by applying the Manning–Strickler equation. In the other three tributaries, we took advantage of the water diversion structures and used weir equations to assess peak discharge. The uncertainties associated with these estimates were evaluated by taking into account the uncertainties affecting the retrieval of maximum flow depth for the weir equations and by using the method described by Amponsah et al. (2016) for the application of the Manning–Strickler equation and are reported in Zaramella et al. (2020, 2023).

Flood hydrographs and ensuing flow-related variables at the sub-reach scale in the channels selected for the analysis of channel widening were obtained by applying the distributed Grid-based runoff simulation (GRIS) (Zaramella et al., 2020; Brenna et al., 2021). GRIS is based on the availability of raster information of the landscape topography and of the soil, geology and vegetation properties. In the model, the Probability Distributed Model approach (PDM; Moore, 2007) is applied on a grid-by-grid way for the spatially distributed representation of runoff generating processes, while a simple description of the drainage system response (Da Ros and Borga, 1997) is used to represent runoff propagation by means of a kinematic model. The PDM model requires the specification of a number of parameters and chiefly the estimation of the maximum storage capacity which yields the spatially distributed soil water storage capacity. The distributed runoff propagation procedure is based on the identification of drainage paths and requires the characterization of hillslope paths and channelled paths as well as the specification of two invariant hillslope and channel velocities, respectively. The hillslope and channelled flow paths are determined by a using drainage threshold area parameter.

The model was implemented over the study area by accounting for uncertainty in the PDM model parameters by using the Generalized Likelihood Uncertainty Estimation (GLUE; Beven and Binley, 2014). In this step, relationships between the PDM model parameters and the lithology of the basin were exploited (Norbiato et al., 2008; Zaramella et al., 2020, 2023) when conditioning the model parameters over the basin upstream from Ponte Mas. The resulting ensemble of simulated model hydrographs was able to bracket the flood observations (both observed hydrographs and indirect estimates of flood peaks) for almost all the study basins (Zaramella et al., 2020, 2023). In particular, model-simulated peak discharges fell within the uncertainty range of post-flood peak discharges in three out of the four catchments analysed for channel widening. Only the model simulation for the Liera river basin overestimated peak discharge (by 14.5 %) with respect to the central value of the post-flood estimates, thus falling immediately outside the uncertainty range. In the remaining part of the work, median flood hydrograph model simulations are reported.

The unit stream power (Bagnold, 1977, 1980) induced by water flow on a streambed is frequently used to predict channel responses to large floods (e.g. Magilligan, 1992; Surian et al., 2016; Yochum et al., 2017). The unit stream power that occurred at the peak of the Vaia flooding was calculated at the sub-reach scale as follows:

$$\omega_{pk} = \frac{\rho g Q_{peak} S}{W} \quad (1)$$

where ρ denotes the water density (1000 kg m^{-3}), g represents the gravity acceleration (9.81 m s^{-2}), S is the sub-reach channel slope (m/m) and W is the channel width (m). The peak discharge (Q_{peak}) was computed by applying the calibrated GRIS model at the sub-reach scale. Given that the actual W at the peak of the Vaia event is unknown, as indicated by Brenna et al. (2021), the unit stream power was calculated two times at each sub-reach using Eq. (1) considering both W_{pre} (ω_{pk}^{pre}: unit stream power calculated using the channel width before the event) and W_{post} (ω_{pk}^{post}: unit stream power calculated using the channel width after the event) as the W.

3.4. Available data on sediment–water flows

Directly monitoring transport processes in mountain streams is often infeasible during floods. A sound alternative is to enquire into the morphological (e.g. shape, surface characteristics and peculiar landforms) and sedimentological (e.g. sorting, texture, stratification and clasts imbrication and orientation) features of related flood deposits, which depend chiefly on flow type at the time of deposition (Postma, 1986). Brenna et al. (2020a) developed a survey protocol for collecting field evidence for classifying flood deposits on the basis of the type of flow through which sediment is deposited (i.e. debris flow, hyperconcentrated flow, debris flood and water flow; see Table S1). Brenna et al. (2020a, 2020b) used this protocol to collect data along the Tegnas Torrent (one of the streams also analysed in this work; Fig. 1), determining, at the sub-reach scale, the sediment–water flows triggered by Vaia along its main stem (Fig. 4). Along the steep T1 reach of the Tegnas Torrent, a longitudinal passage from debris flow to debris flood and water flow occurred during the Vaia event at the first three sub-reaches, followed by debris flows that affected two sub-reaches (i.e. T1.4 and T1.5) and debris flood occurring at one sub-reach (i.e. T1.6). In the downstream sector of the Tegnas main stem (i.e. reaches T2–T6), water flow occurred in most of the sub-reaches, but debris floods were triggered during the Vaia flooding at sub-reaches T2.4, T4.1, T4.2, T6.2 and T6.3. At sub-reaches T3.1, T3.2, T7.1 and T7.2, Vaia deposits were not preserved at the time of the survey (Brenna et al., 2020a).

Most of the Vaia deposits were removed or altered during the emergency interventions carried out in the weeks after the flood, thereby obliterating the original features of the sediments. Moreover, some minor floods that occurred following the Vaia event reworked the deposits. For these reasons, the sediment–water flows triggered by the Vaia storm could be defined on the basis of flood deposit surveys by Brenna et al. (2020a, 2020b) only for the Tegnas Torrent, where field survey efforts were focused after the flood.

3.5. Analysis of controlling factors for channel widening

The controlling factors for channel widening were investigated at the sub-reach scale using multiple-explanatory models, with WR as the dependent variable and five independent control variables. In detail, three geomorphic (S, CI and AS) and two hydraulic (ω_{pk}^{pre} and ω_{pk}^{post}) variables were considered. As in Surian et al. (2016), the regressions were run on the entire data set (i.e. the 117 sub-reaches defined in this work and the 27 sub-reaches of the Tegnas Torrent) and two sub-sets created from the division of the sample on the basis of channel slope (i.e. $S > 4\,\% =$ steep channels, $S < 4\,\% =$ non-steep channels). To further explore the relationships found through this procedure, single-explanatory regression models were estimated to determine the association between WR and the significant controlling factors identified via the multiple regressions. Statgraphics Centurion XVIII (https://www.statgraphics.com/how-to-guides) was used for the statistical analysis.

The data were analysed to pinpoint sub-reaches characterised by major channel changes. We specifically regarded intensely widened sub-reaches as those characterised by remarkably high WR values, that is, sub-reaches where the observed WR exceeded the 85th percentile of the distribution of the WR values. This threshold was arbitrarily selected but enabled us to identify the sub-reaches where widening was intense. Our aim was to investigate the existence of relationships between such intense widening and the local occurrence of debris flood instead of ordinary water flow that mobilized the bed material in a channel sub-reach. For the Tegnas Torrent, the occurrence of debris floods during the Vaia storm was determined from the field-based classification of

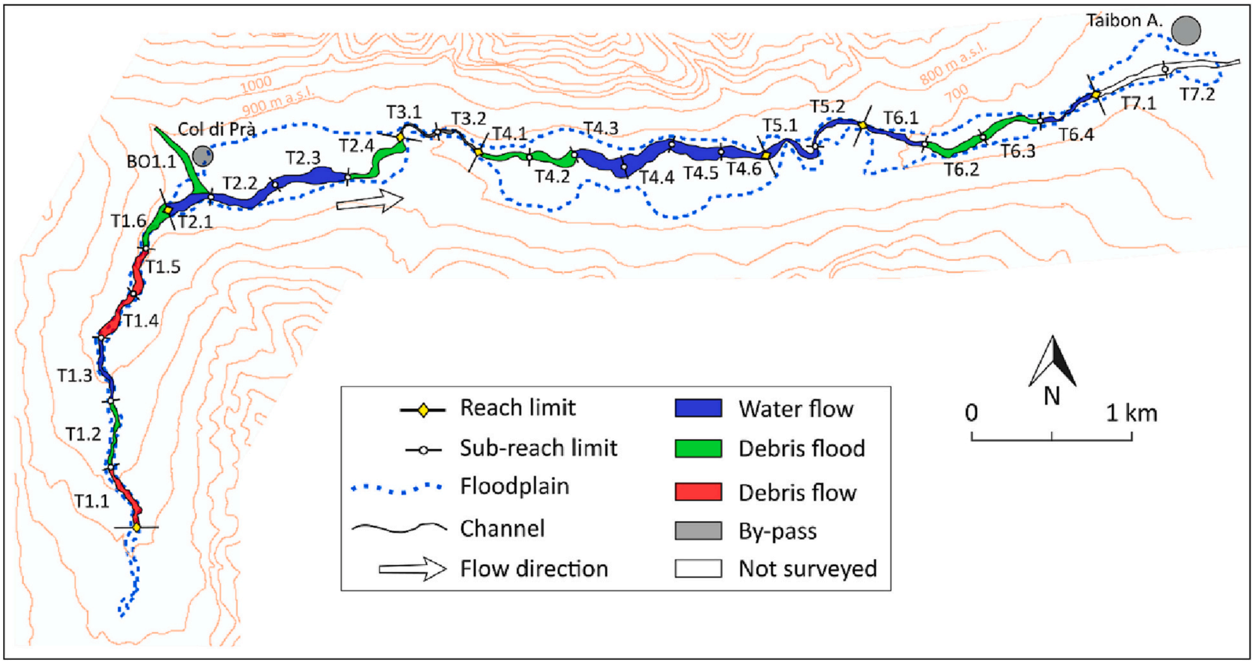

Fig. 4. Sediment–water flows occurring during the Vaia flooding along the Tegnas Torrent [modified from Brenna et al., 2020a]. Details about the transport processes and their relationships with hydraulic forcing and channel dynamics are available in Brenna et al. (2021).

transport processes performed by Brenna et al. (2020a) (Fig. 4). On the contrary, no field data and deposit interpretations were available for the Cordevole, Pettorina, Corpassa and Liera streams. For the sub-reaches of these four streams characterised by intense channel widening (i.e. sub-reaches where the WR exceeded the 85th percentile of the distribution of the WR values), the possible occurrence of debris flood instead of water flow during the high-magnitude Vaia flooding was inferred from the presence of the conditions necessary for debris flood occurrence as formulated by Brenna et al. (2021) from the analysis performed in the Tegnas Torrent, which are:

(1) High hydraulic forcing, with ω_{pk}^{pre} exceeding about 5000 Wm^{-2}: This condition is necessary—although alone not sufficient—for the occurrence of debris flood type 1 (debris flood triggered by the exceedance of a critical stress acting on a streambed given a severe flood).
(2) Debris flow tributaries delivering a large amount of sediment into a receiving stream during the event: This condition is necessary—although alone not sufficient—for the occurrence of debris flood type 2 (debris flood generated by the progressive dilution of a debris flow by sedimentation or the injection of water). This condition was evaluated by observing the configuration of tributaries before and after the flood on the available sets of images (i.e. 2015 and 2018 or 2019 images) and their connection with the main stem of a stream (Fig. 3c and d), as well as through some field observations of the tributaries of the Liera Torrent (Macchi et al., 2022).

For each intensely widened sub-reach of the Cordevole, Pettorina, Corpassa and Liera streams, we evaluated the presence or absence of the aforementioned conditions necessary for debris flood occurrence. In their absence, the sediment-water flow locally triggered during the Vaia storm was interpreted as water flow. On the contrary, at intensely widened sub-reaches where ω_{pk}^{pre} exceeded about 5000 Wm^{-2} (condition 1) and/or debris flow tributaries delivered a large amount of sediment to a receiving stream (condition 2), we inferred that debris floods could reasonably have locally occurred during the Vaia flooding.

4. Results

4.1. Channel widening

Widening occurred in most of the studied channels (Table 2 and Fig. 5). The largest W_{pre} was found in the Cordevole River, whose WR never exceeded 2.45 (sub-reach CD3.5). The largest widening in absolute terms occurred at sub-reach CD8.7 along the Cordevole River and was equal to 90.3 m. The Tegnas and Corpassa torrents had similar W_{pre}, but remarkably greater widening occurred in the Tegnas Torrent (maximum widening in absolute terms of 37.2 m at sub-reach T4.3). By contrast, the channel width of the Corpassa Torrent did not change during the Vaia event, except for sub-reach CP2.3, which was characterised by widening in absolute terms of 8.0 m and a WR = 1.84. The two streams with low W_{pre} underwent the greatest widening in terms of WR (Table 2), with maximum widening in absolute terms of 45.6 and 42.6 m for Liera (sub-reach L5.2) and Pettorina (sub-reach P3.3), respectively. An inverse relationship was found between WR and W_{pre} (Fig. 5b), which was expected because of the spurious correlation between these variables. Nonetheless, a broad spectrum of WRs (ranging from 1 up to about 16) occurred in the narrower sub-reaches, whereas sub-reaches having a W_{pre} higher than 10 m never experienced a WR higher than 3.5 (Fig. 5b).

Table 2
Summary of average channel widths before (W_{pre}) and after (W_{post}) the Vaia flood and the WR determined at the sub-reach scale for the studied rivers. The Tegnas Torrent data were obtained from Brenna et al. (2021). The maximum and minimum values of each parameter are presented in brackets. Detailed morphological data on each sub-reach of each river are available in Tables S2, S3, S4, S5 and S6 of the Supplementary Material.

River	Average W_{pre} (m)	Average W_{post} (m)	Average WR
Cordevole	79.6 [18.1–226.6]	110.8 [33.2–308.8]	1.55 [1.07–2.45]
Corpassa	23.4 [9.5–33.2]	23.3 [13.7–30.2]	1.05 [0.84–1.84]
Pettorina	7.3 [2.8–15.8]	19.9 [7.4–47.2]	3.16 [1.25–10.27]
Tegnas	18.3 [4.3–59.0]	37.4 [9.4–77.5]	2.48 [1.21–6.10]
Liera	4.8 [2.5–12.3]	23.2 [6.3–52.7]	5.34 [1.48–15.84]

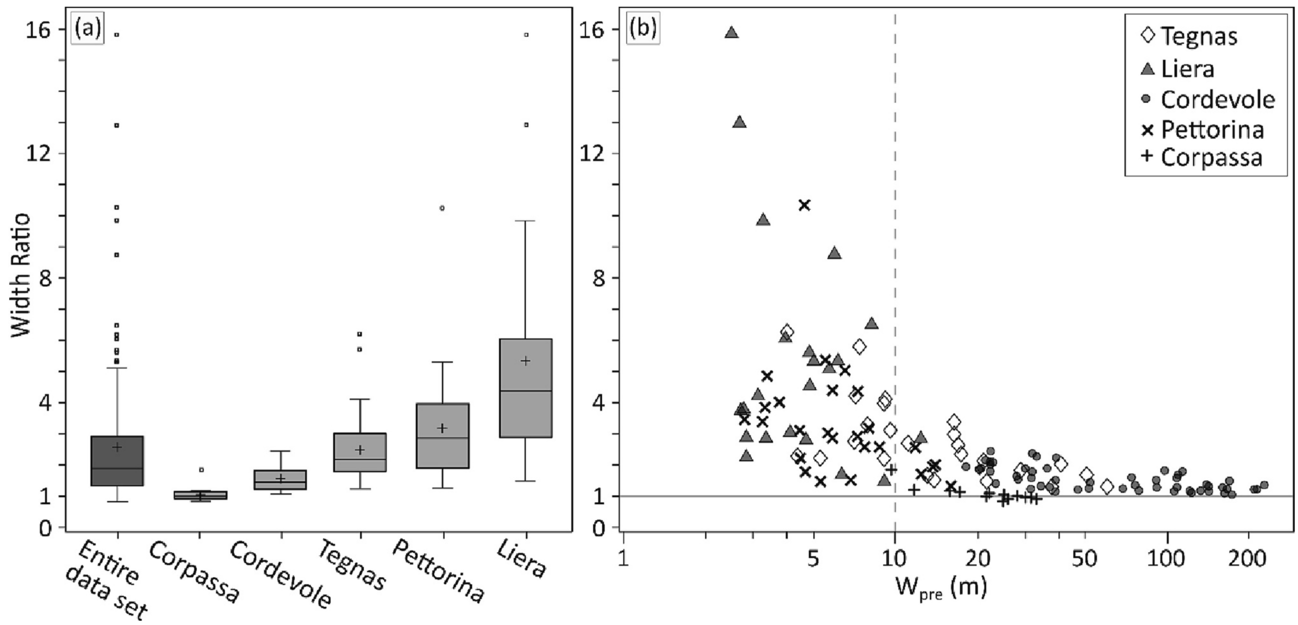

Fig. 5. (a) WR range calculated for the sub-reaches of the studied rivers. The box ends represent the 25th and 75th percentiles, the whisker ends denote the 10th and 90th percentiles and the horizontal lines and crosses indicate the median and mean values, respectively. In (b), we see the WR magnitude against channel width before the flood (W_{pre}) calculated at the sub-reach scale. The threshold of W_{pre} = 10 m, above which WR was always lower than 3.5, is represented with a dashed line.

4.2. Peak discharge and unit stream power

The estimated unit peak discharge [$q_{peak} = Q_{peak}/A$ (m^3s^{-1} km^{-2})] obtained along all the sub-reaches was highly variable, even in catchments of similar areas. This phenomenon was due to the large precipitation gradients characterising the convective band occurring on October 29 (Fig. 2b), which triggered peak flows. Table 3 presents the results of the hydrological analysis of flood responses, including the event-cumulative precipitation [P (mm)]; the convective phase-cumulative precipitation [P_{conv} (mm)], occurring over the period 17:00 to 20:00 CET on 29 October 2018; the peak discharge [Q_{peak} (m^3s^{-1})]; and the unit peak discharge [q_{peak} (m^3s^{-1} km^{-2})]. The convective band elongated along the SE–NW direction affected the Tegnas, Liera and Pettorina river basins in a specific manner. The event-cumulative precipitation for these catchments ranged from 352 to 552 mm, with the cumulative precipitation during the convective phase ranging from 62 to 97 mm. These three basins generated the highest unit peak discharges, which ranged from 2.40 to 3.48 m^3s^{-1} km^{-2}. The highest unit peak discharge was observed in the Tegnas, consistent with the large event precipitation and the minimal permeable geology of the basin. Interestingly, despite the abundant precipitation and small catchment size of the Corpassa river basin, it exhibited the lowest unit peak discharge. The permeable lithology (i.e. karstified and fractured dolostone and limestone) of this catchment likely magnified the infiltration losses in the basin.

Table 3
Hydrological analysis of the flood responses along the sub-reach of each river characterised by the highest unit peak discharges. A: drainage area; P: total event precipitation (mm); P_{conv}: total convective precipitation (mm); Q_{peak} (m^3s^{-1}): peak discharge; and q_{peak} (m^3s^{-1} km^{-2}) unit peak discharge. Detailed and complete discharge data on each sub-reach of each river are available in Tables S2, S3, S4, S5 and S6 of the Supplementary Material.

Catchment	Sub-reach	A (km^2)	P (mm)	P_{conv} (mm)	Q_{peak} (m^3s^{-1})	q_{peak} (m^3s^{-1} km^{-2})
Pettorina	P3.4	44.6	352	69	107	2.40
Liera	L6.2	39.9	405	62	109	2.74
Corpassa	CP2.1	24.8	460	42	30	1.20
Tegnas	T4.4	41.3	552	97	144	3.48
Cordevole	CD5.3	610.7	395	48	1247	2.04

The unit stream power of each sub-reach before and after the flood—ω_{pk}^{pre} and ω_{pk}^{post} (Wm^{-2}), respectively—were computed using the relationship expressed in Eq. (1). As reflected by the generalized channel widening (Fig. 5a), the ω_{pk}^{pre} values were always considerably higher than the ω_{pk}^{post} values, except in the Corpassa Torrent where widening was extremely low (Fig. 6). The highest ω_{pk} values calculated on the basis of W_{pre} were those obtained for the Liera and Pettorina torrents, intermediate values were derived for the Tegnas and Cordevole rivers and a ω_{pk}^{pre} commonly lower than approximately 1800 Wm^{-2} was calculated for the Corpassa Torrent. The ω_{pk}^{post} values were similarly distributed, except in the Pettorina Torrent, which experienced a substantially higher ω_{pk}^{post} compared with that of the Liera Torrent given its relatively lower widening (Figs. 5a and 6).

4.3. Analyses of controlling factors and roles of flow types in channel widening

In the multiple regression analyses conducted to identify the most significant controlling factors for channel widening, WR served as the dependent variable, and S, CI, AS, ω_{pk}^{pre} and ω_{pk}^{post} as the control variables. We determined three regression equations [Eqs. (2), (3) and (4)], each of which including only one of the variables related to stream power (S, ω_{pk}^{pre} and ω_{pk}^{post}), to analyse the entire data set (144 sub-reaches), the steep channel sub-set (63 sub-reaches) and the non-steep channel sub-set (81 sub-reaches) (Table 4). All the regression models were significant ($p <$ 0.001) and characterised by moderate performance metrics, but the best model for the three data sets was the one that incorporated ω_{pk}^{pre} as a control variable (i.e. model 3 in Table 4). A backward stepwise regression procedure applied to model 3 enabled us to formulate the following equations intended to describe WR as a function of the significant control variables for the three data sets:

$$WR = 1.09 + 0.066\ CI + 0.00012\ \omega_{pk}^{pre} \quad (2)$$

$$WR = 1.19 + 0.078\ CI + 0.00010\ \omega_{pk}^{pre} \quad (3)$$

$$WR = 1.15 + 0.045\ CI + 0.00014\ \omega_{pk}^{pre} \quad (4)$$

Eqs. (2), (3) and (4) refer to the entire data set, the steep channel sub-

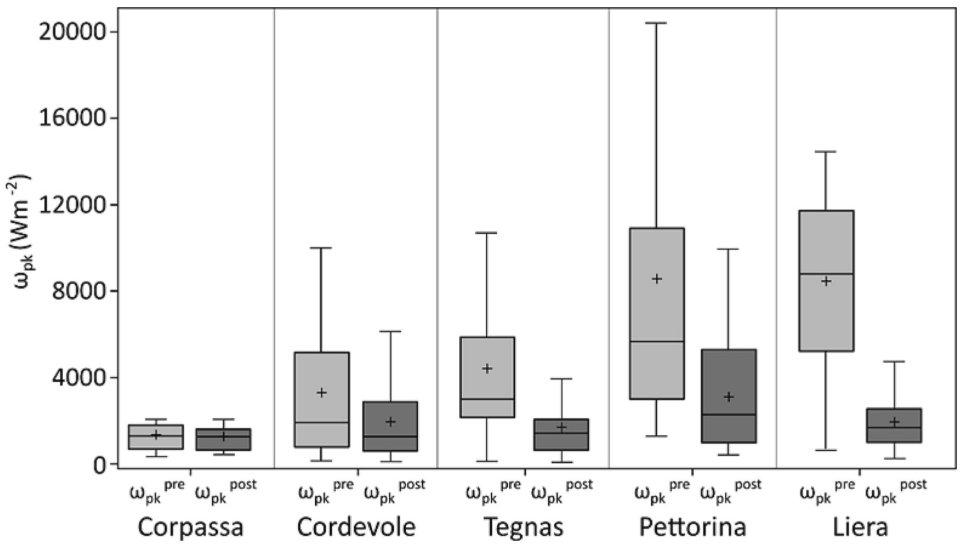

Fig. 6. Ranges of ω_{pk}^{pre} (light grey) and ω_{pk}^{post} (dark grey) calculated for the sub-reaches of the studied rivers. The box ends represent the 25th and 75th percentiles, the whisker ends denote the 10th and 90th percentiles and the horizontal lines and crosses indicate the median and mean values, respectively. Detailed hydraulic data on each sub-reach of each river are available in Tables S2, S3, S4, S5 and S6 of the Supplementary Material.

Table 4
Multiple-explanatory models of regression between WR and the control variables. The models with the best statistical performance are presented in bold typeface.

		Model 1	Model 2	Model 3
Entire data set		$R^2 = 0.37$ *p*-value <0.001 Std. Err. = 1.73 p-value	$R^2 = 0.37$ *p*-value <0.001 Std. Err. = 1.73 p-value	**$R^2 = 0.44$ p-value < 0.001 Std. Err. = 1.64** p-value
	CI	< 0.001	< 0.001	< 0.001
	AS	0.0072	0.0729	0.1376
	S	0.5265	–	–
	ω_{pk}^{post}	–	0.4463	–
	ω_{pk}^{pre}	–	–	< 0.001
Steep channels		$R^2 = 0.41$ p-value <0.001 Std. Err. = 2.20 p-value	$R^2 = 0.41$ p-value <0.001 Std. Err. = 2.20 p-value	**$R^2 = 0.45$ p-value < 0.001 Std. Err. = 2.13** p-value
	CI	< 0.001	< 0.001	< 0.001
	AS	0.5718	0.1938	0.2624
	S	0.1016	–	–
	ω_{pk}^{post}	–	0.1572	–
	ω_{pk}^{pre}	–	–	< 0.001
Nonsteep channels		$R^2 = 0.41$ p-value <0.001 Std. Err. = 1.05 p-value	$R^2 = 0.30$ p-value <0.001 Std. Err. = 1.14 p-value	**$R^2 = 0.44$ p-value < 0.001 Std. Err. = 1.05** p-value
	CI	< 0.001	< 0.001	< 0.001
	AS	0.1537	0.0263	0.1539
	S	< 0.001	–	–
	ω_{pk}^{post}	–	0.5753	–
	ω_{pk}^{pre}	–	–	< 0.001

set and the non-steep channel sub-set, respectively. AS was consistently excluded from the models ($p > 0.05$), and CI and ω_{pk}^{pre} significantly defined the WR of both steep and non-steep sub-reaches ($p < 0.05$). The R^2 values of the three models were almost identical, while the standard error obtained for the steep channel sub-set was higher than that of the non-steep channel sub-set (Table 4). Five steep sub-reaches of the Liera Torrent (L3.1, L3.2, L4.1, L4.4, L5.2), one steep sub-reach of the Tegnas (BO1.1) and one non-steep sub-reach of the Pettorina Torrent (P3.3) were characterised by anomalous positive residuals (residual >2) between the WR predicted by the regression models and the observed WR.

The two most important controlling factors (CI and ω_{pk}^{pre}) were used to develop single-explanatory regression models for the examination of the entire data set and two sub-sets (Fig. 7). The best regression models among the 27 tested ones were automatically selected by the statistical software employed in this work on the basis of statistical metrics (i.e. R^2, standard error and correlation coefficient). WR was clearly related to CI in both steep ($R^2 = 0.54$; Fig. 7c) and non-steep ($R^2 = 0.42$; Fig. 7e) channels and to ω_{pk}^{pre}, but the latter association was stronger in steep channels ($R^2 = 0.63$; Fig. 7d) than in non-steep channels ($R^2 = 0.29$; Fig. 7f).

Because the regression models for all the data sets considered in the analyses showed significant relationships among WR, CI and ω_{pk}^{pre} (Table 4 and Fig. 7), the following investigations exclusively focused on the entire data set centred on the distribution of WR. The 85th percentile of WR distribution was 3.96 and covered 123 sub-reaches out of the total 144 (Fig. 7a and b). The remaining 21 sub-reaches have WR in the range between 4.10 and 15.84 and pointed to channel locations where intense widening occurred during the flood. These sub-reaches are located in the Liera (12 sub-reaches), Pettorina (six sub-reaches) and Tegnas (three sub-reaches) torrents (Table 5). All intensely widened sub-reaches were characterised by low lateral confinement (CI > 8.2; Fig. 7a). No such widening took place in the sub-reaches of the Cordevole River and Corpassa Torrent.

The results of Brenna et al. (2020a) (Fig. 4) showed that at the three sub-reaches of the Tegnas Torrent that were characterised by major channel widening (T4.1, T6.2 and BO1.1), debris flood was the flow type triggered during the Vaia event. No direct observations or flood deposit features attesting to the sediment–water flow types occurring during the event were available for the Liera and Pettorina torrents. Restoration work carried out in the weeks after the October 2018 flood (sediment removal and the reshaping of channel cross-sections) obliterated evidence that could have permitted the recognition of the water–sediment transport processes occurring in these channels. For this reason, we focused on the 18 sub-reaches of the two aforementioned torrents, where intense widening transpired, to evaluate the local presence or absence of the conditions necessary for the occurrence of a debris flood ($\omega_{pk}^{pre} > 5000$ Wm^{-2} —condition 1— and/or debris flow tributaries delivering a large amount of sediment to a receiving stream —condition

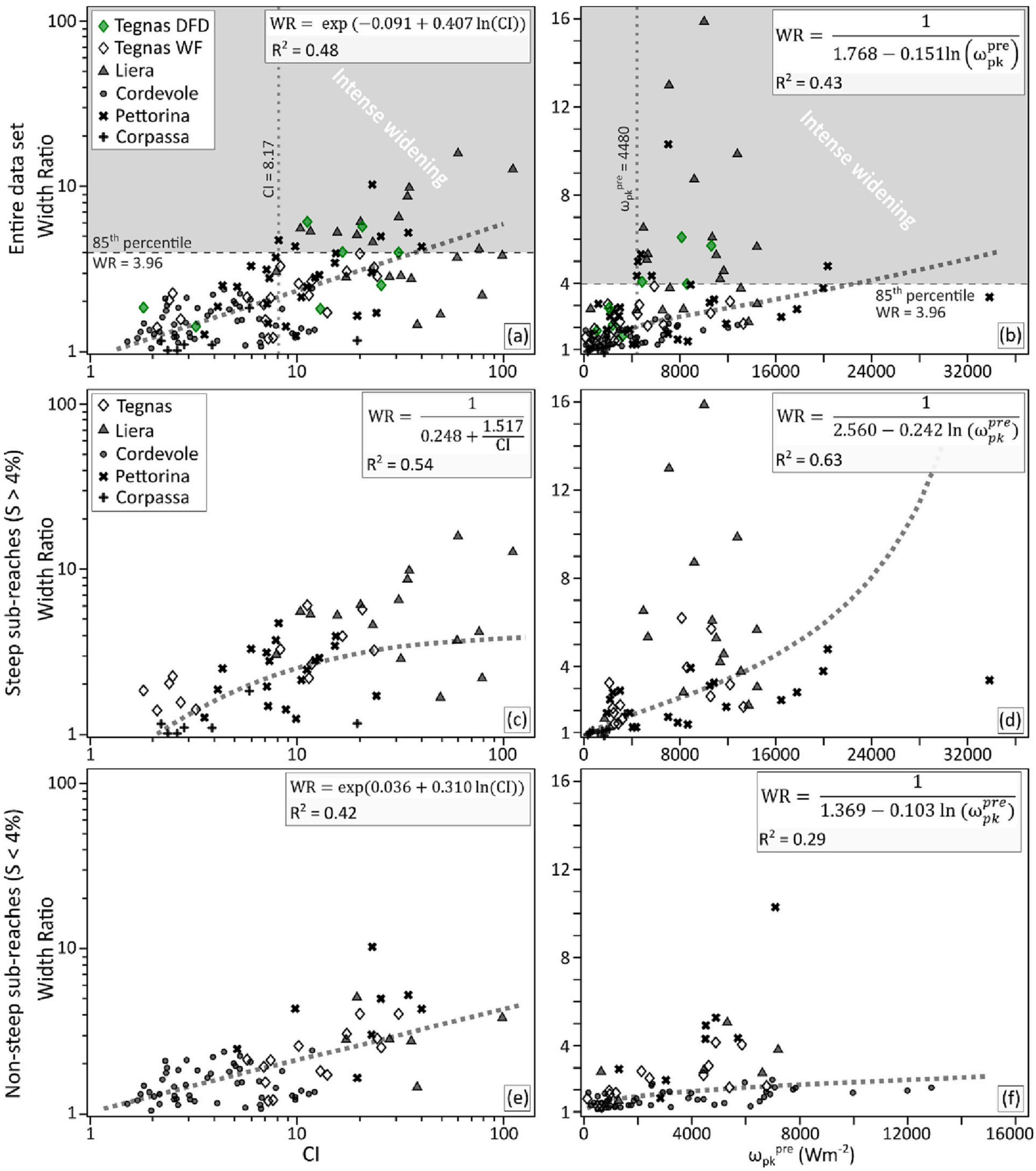

Fig. 7. Single-explanatory models of regression between WR and the controlling factors (CI: confinement index; ω_{pk}^{pre}: unit stream power calculated using channel width before the event) for the entire data set (a and b), steep sub-reaches (c and d) and non-steep sub-reaches (e and f). Regressions are represented by the dotted lines. In plots (a) and (b), sub-reaches of the Tegnas Torrent are distinguished on the basis of the sediment–water flow types occurring during the Vaia event (WF: water flow; DFD: debris flood), as reported by Brenna et al. (2020a).

2—; Brenna et al., 2021) during a high-magnitude hydrological event such as the Vaia flooding. The ω_{pk}^{pre} estimated for the 18 sub-reaches was always high, ranging from 4480 Wm^{-2} at P3.5 to 20,402 Wm^{-2} at P2.3 (Table 5 and Fig. 7b). Sediment input from debris flow tributaries flowing into the main stem at a sub-reach where intense widening occurred or from debris flow tributaries flowing immediately upstream (i.e. up to a few tens of meters from the upstream limit of the sub-reach) was recognized at six sub-reaches of the Liera Torrent and four sub-reaches of the Pettorina Torrent (Table 5). Conditions 1 or 2 required for the occurrence of a debris flood (see Section 3.5) were present in all intensely widened sub-reaches, with concurrent occurrence of both conditions 1 and 2 in ten out of the 18 intensely widened sub-reaches (Table 5). On the basis of these results, we inferred that debris floods could reasonably have occurred during the Vaia flooding at these 18 channel sites.

Table 5

Sub-reaches affected by intense widening during the Vaia flooding and their main morphological (slope), hydraulic (ω_{pk}^{pre}: unit stream power calculated using the channel width before the event) and sedimentary characteristics (presence of debris flow tributaries delivering a large amount of sediment to a receiving stream). For each sub-reach, the WR expected on the basis of the best regression models derived for steep [Eq. (3)] and non-steep [Eq. (4)] channels, the WR actually occurring during the flood (observed WR) and relative differences between these two (Δ Expected – Observed, in %) are reported as well. *: sub-reach of the Tegnas Torrent, for which the occurrence of debris flood during the Vaia event was determined by Brenna et al. (2020a); +: sub-reaches characterised by anomalous positive residuals (residual >2) between the WR predicted by the regression models in Table 4 and the observed WR.

River	Sub-reach	Slope (%)	ω_{pk}^{pre} (W m^{-2})	Debris flow input	Expected WR	Observed WR	Δ Expected - Observed (%)
Tegnas	T4.1*	2.63	4872	Yes	3.22	4.10	+ 27
	T6.2*	4.90	10,625	No	3.86	5.69	+ 47
	BO1.1*+	6.30	8148	No	2.86	6.10	+ 113
Liera	L3.1+	5.45	9972	Yes	6.87	15.84	+ 131
	L3.2	4.03	7048	No	10.50	12.95	+ 23
	L3.3	6.80	11,308	No	4.16	4.21	+ 1
	L4.1+	6.44	12,802	Yes	5.17	9.85	+ 90
	L4.2	6.26	10,623	No	3.82	6.06	+ 59
	L4.3+	4.30	5293	Yes	2.93	5.34	+ 82
	L4.4+	3.81	5279	Yes	2.77	5.10	+ 85
	L4.5	6.12	10,945	Yes	3.18	5.29	+ 66
	L5.1	6.13	11,674	No	4.16	4.56	+ 10
	L5.2+	5.52	9225	Yes	4.74	8.75	+ 85
	L5.3	4.01	4939	No	4.10	6.50	+ 59
	L6.2	6.35	14,371	No	3.44	5.64	+ 64
Pettorina	P2.3	9.45	20,402	Yes	4.37	4.77	+9
	P3.3+	3.59	7086	Yes	3.18	10.27	+ 223
	P3.4	2.78	4512	Yes	2.92	4.97	+ 70
	P3.5	2.48	4480	Yes	3.58	4.32	+ 21
	P3.6	2.48	4822	No	3.37	5.29	+ 57
	P4.5	3.62	5676	No	2.38	4.31	+ 81

5. Discussion

5.1. Channel widening in the rivers of the Cordevole river basin

During the Vaia event, comparable average channel responses took place along the Tegnas, Pettorina and Liera torrents, which exhibited a mean WR ranging from 2.5 to 5.3 (Fig. 5a). Lower average widening occurred along the Cordevole River (WR = 1.6). Its average channel width before the flood was considerably higher than the W_{pre} of the other analysed streams (Table 2): 52 sub-reaches out of 53 in the Cordevole River had a $W_{pre} > 20$ m and registered a maximum WR that never exceeded 2.5 (Fig. 5b). In accordance with the findings of previous studies (e.g. Righini et al., 2017; Ruiz-Villanueva et al., 2018), the current results indicate that, with respect to WR, low widening is typically associated with a high initial channel width. Similarly limited widening occurred at six Tegnas Torrent sub-reaches, which had a $W_{pre} > 20$ m (Fig. 5b and Table S2). An initial channel width of about 20 to 30 m could serve as an approximate threshold for widening that likely does not exceed a WR of 2 to 2.5 also in response to high-magnitude hydrological forcing. Such relatively low WR values are related to the lower unit stream power generated by water discharge flowing into a wide river channel compared with that flowing into a narrow section [see Eq. (1)].

Even lower widening occurred along the Corpassa Torrent (average WR = 1.1), where eight sub-reaches experienced no widening during the flood, and the remaining seven had a WR never exceeding 1.8 (Fig. 5). Similar to what was observed for the majority of the Cordevole River sub-reaches and some of the Tegnas Torrent sub-reaches, such a limited response to the flood can be partially ascribed to the high W_{pre} of the Corpassa Torrent (with only four out of 15 sub-reaches having an initial width < 20 m; Tables 2 and S5 and Fig. 5b). This limited morphological response seemed to have been determined also by the low hydrological forcing that occurred in the Corpassa catchment during the event. The max q_{peak} was equal to 1.20 m^{3}s^{-1} km^{-2}—a value remarkably lower than the max q_{peak} estimated for the other catchments examined in this study (Table 3). Such a value is low compared with the unit peak discharges commonly associated with high-intensity European and Mediterranean floods (Amponsah et al., 2018), and it drove the ω_{pk} to vary from 400 to 2000 Wm^{-2} along the channel (Table S5).

Taking into account the peculiarities characterising each catchment discussed above, our results confirmed that CI and ω_{pk}^{pre} are significant morphological and hydraulic factors for explaining channel widening in response to high-magnitude floods in terms of WR (Table 4), in accordance with the findings of Surian et al. (2016) and Scorpio et al. (2018). The statistical metrics (i.e. *p*-value, standard error and R^2) of the best models derived with regard to the association among WR, CI and ω_{pk}^{pre} through simple and multiple regressions (Table 4, Fig. 7) are comparable with those obtained in the aforementioned studies.

5.2. Intense channel widening and fluid gravity flows

The regression models devised in this study to explore the relationships between channel widening and morphological and hydraulic constraints were satisfactory from a statistical point of view. Nevertheless, the use of the controlling factors (CI and ω_{pk}^{pre}) generated a broad spectrum of WR values along the studied stream network, particularly under high hydraulic forcing and low channel confinement (Fig. 7). We specifically focused on channel sites where intense widening occurred, defined as sub-reaches where the observed WR was higher the 85th percentile of the distribution of the WR values, that is, sub-reaches having a WR higher than 3.96.

Intense channel widening was found along the main stems of the Tegnas, Liera and Pettorina torrents at 3, 12 and 6 sub-reaches, respectively (Fig. 7). At the three sub-reaches of the Tegnas Torrent, debris flood was the flow type triggered during the Vaia event (Fig. 4). The 18 intensely widened sub-reaches of the Liera and Pettorina torrents were characterised by a ω_{pk}^{pre} that was always >4480 Wm^{-2} (Table 5)—a value very close to the threshold of 5000 Wm^{-2} identified as necessary for debris flood type 1 (Church and Jakob, 2020) to occur in the Tegnas Torrent (Brenna et al., 2021). They were also typified by the presence of numerous debris-flow tributaries delivering substantial volumes of sediment into them (Table 5), which is a condition necessary for debris flood type 2 (Church and Jakob, 2020; Brenna et al., 2021) to take place. High ω_{pk}^{pre} and debris flow input occurred concurrently at six and four intensely widened sub-reaches of the Liera and Pettorina torrents, respectively. On the basis of these characteristics, it is highly likely that during the Vaia event, debris flood was the flow type responsible for sediment mobilization at these Liera and Pettorina sub-reaches instead of ordinary water flow. This inference cannot be confirmed by field evidences but it was considered robust since it takes into account for the presence—or absence—of conditions 1 and 2 necessary for debris flood occurrence (see Section 3.5) that were drawn up by Brenna et al. (2021) for a mountain stream (the Tegnas Torrent) that belongs to the same geographical region of the Liera and Pettorina streams (Fig. 1) and shares with them a number of sedimentological, geomorphological and morphometric characteristics (Table 1). Moreover, conditions 1 and 2 were formulated by analysing the transport processes triggered by the same hydrological event (the Vaia storm) whose effects in terms of transport processes were analysed in the Liera and Pettorina streams.

Despite the high channel slope of the Corpassa Torrent, none of its

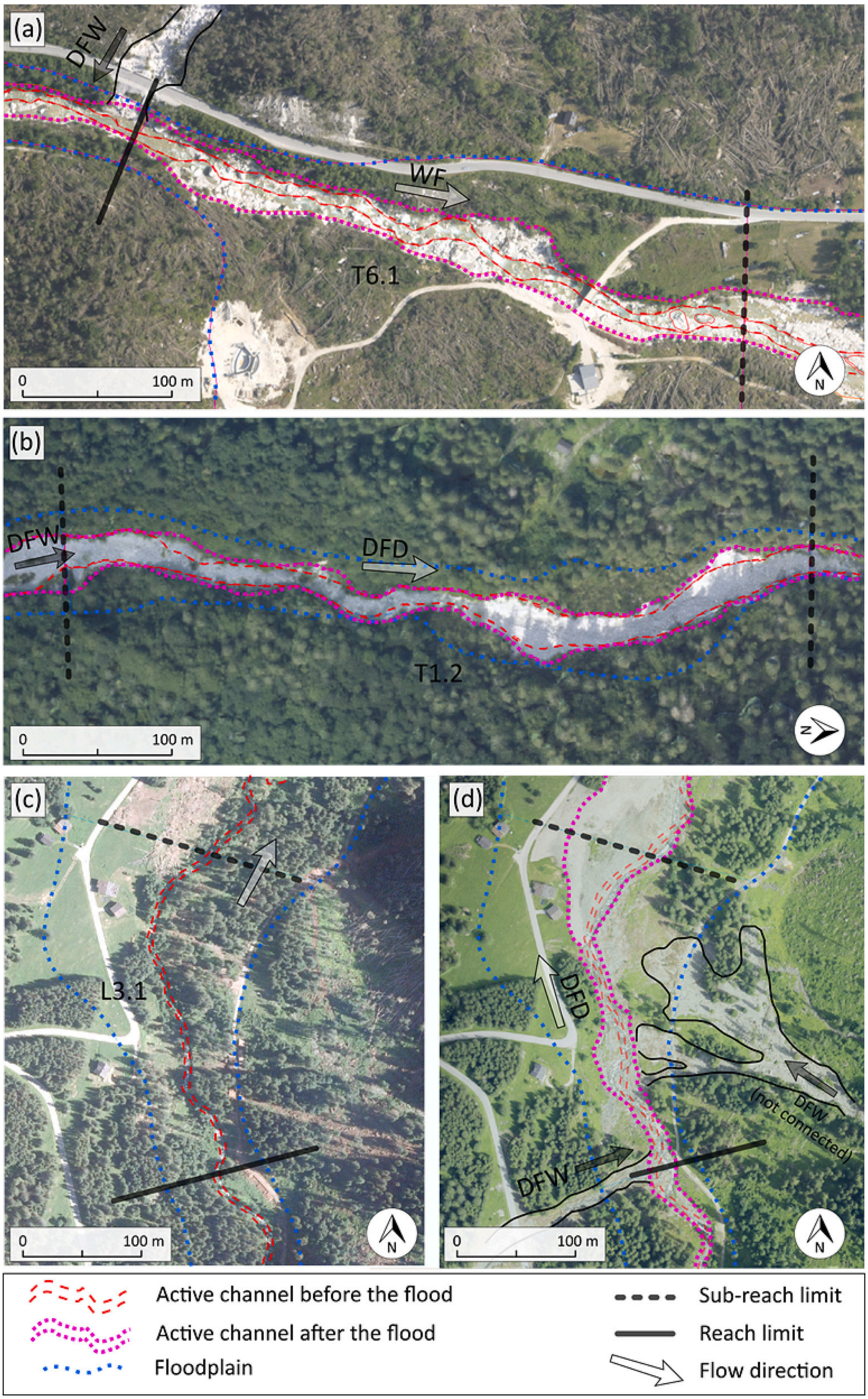

Fig. 8. Geomorphic processes occurring at sub-reaches of the studied network during the Vaia event (a and b: sub-reaches T6.1 and T1.2 of the Tegnas Torrent, respectively; c and d; sub-reach L3.1 of the Pettorina Torrent before and after the flood, respectively). T6.1 is an example of sub-reach where, despite the presence of conditions allowing for potential debris flood occurrence, water flow took place during the Vaia event. T1.2 is an example of sub-reach where, despite debris flood triggering during the Vaia strom, the boundary conditions locally characterising the channel precluded the occurrence of intense widening. L3.1 is an example of a channel site likely affected by debris flood and experiencing intense widening. DFW: debris flow; DFD: debris flood; WF: water flow.

sub-reaches exhibited the conditions necessary for debris flood to take place; this phenomenon stemmed from the relatively low convective precipitation induced by the storm at this catchment (Table 3), which caused moderate flooding and hydraulic forcing acting on the streambed. Additionally, no tributary generated debris flows connected to the main stem of the Corpassa Torrent.

The Cordevole River is a large mountain river with a pre-flood channel width that is always larger than 20 m; this value extends up to 100 to 200 m along several sub-reaches of the river's course downstream from Agordo (Figs. 1 and 2a and Table S6). These characteristics render the occurrence of a debris floods along its main stem extremely difficult, also in response to an extreme flood (i.e. a recurrence interval higher than 100 years). It is highly probable that in the Corpassa Torrent and Cordevole River, the transport processes activated during the Vaia event remained in the range of water flow accompanied by bedload transport.

All the 21 sub-reaches for which intense widening was observed were affected by debris flood during the Vaia event (i.e. three sub-reaches of the Tegnas Torrent; Fig. 4) or were characterised by the presence of the conditions necessary for debris flood occurrence in response to a severe flood (i.e. 18 sub-reaches of the Liera and Pettorina; Table 5). Accordingly, we can reliably conclude that the occurrence of debris flood instead of ordinary water flow was a primary driver of intense widening locally affecting a channel during high-magnitude floods. Moreover, the results of Brenna et al. (2021) highlighted that the sub-reaches of the Tegnas Torrent affected by debris flood during the Vaia storm experienced channel widening that was two to three times larger than that exhibited by sub-reaches where water flow occurred at the same unit stream power. From a process point of view, these findings agree with the characteristics typifying the sediment dynamics underlying debris floods. Church and Jakob (2020) recently clarified that a debris flood can cause the full mobilization of an entire streambed, with grains of almost all sizes forming the bed transported under conditions of full mobility. During such an extreme transport condition, the streambed is in fact exposed to live bed conditions, thereby exerting profound effects on channel planforms, such as morphological re-arrangement and extensive bank erosion (Church and Jakob, 2020).

Some sub-reaches characterised by the presence of conditions necessary for debris flood occurrence did not undergo intense widening, as defined in this work, during the Vaia event. This behaviour can be explained by two hypotheses: first, debris flood did not occur during the Vaia storm despite the presence of conditions conducive to its occurrence, and second, debris flood occurred, but some local boundary conditions prevented the channel from widening intensely. The first hypothesis is supported by the fact that the conditions necessary for debris flood occurrence (i.e. $\omega_{pk}^{pre} > 5000$ Wm^{-2} and/or debris flow tributaries delivering a large amount of sediment to a receiving stream; Brenna et al., 2021) do not necessarily imply that such an intense transport phenomenon occurs, as these conducive conditions are required but alone not sufficient for debris flood activation. A sub-reach that can be definitively described as falling in this first hypothesis is T6.1 in the Tegnas Torrent, where the flow type activated during the Vaia event was water flow (Fig. 4; Brenna et al., 2020a) in response to extremely high ω_{pk}^{pre} and debris flow input from a steep tributary (Fig. 8a); this effect is probably due to the presence of mega-boulders in the channel that limited the overall mobility of streambed material locally precluding debris flood to occur (Brenna et al., 2021). At T6.1, the channel widened 3.19 times the initial width, that is −25 % with respect to the WR of 4.24, which was expected on the basis of Eq. (3) with a $\omega_{pk}^{pre} = 12{,}242$ Wm^{-2} and a CI = 23.41. The other sub-reaches of the investigated stream network where a similar situation could have happened during the Vaia event are, for instance, P1.7 of the Pettorina Torrent (Table S3) and L2.1 of the Liera Torrent (Table S4). The second hypothesis implies that debris floods do not always cause intense channel widening. At sub-reach T1.2 of the Tegnas Torrent (Fig. 8b), for example, debris flood occurred during the Vaia event (Fig. 4), but the observed WR of 1.41 was in line with the WR of 1.73 expected on the basis of Eq. (3) under a $\omega_{pk}^{pre} = 2919$ Wm^{-2} and a CI = 3.21. Debris flood did not produce intense widening at the sub-reach because of channel confinement, the mega-boulders forming the narrow floodplain adjacent to the channel and the dense vegetation cover that inhibited bank erosion (e.g. Beeson and Doyle, 1995). Other conditions limiting bank erosion and, consequently, intense channel widening in debris flood conditions were widespread bank protections as occurred for instance at sub-reach P3.2 of the Pettorina Torrent where AS = 82 % (Table S3) and the high natural confinement induced by rock slopes for sub-reaches P2.1 to P2.4 of the Pettorina Torrent (Table S3), where the stream flows in a narrow gorge. The absence of elements that limit channel widening by preventing bank erosion is a condition that allows intense widening in case of debris flood occurrence. Accordingly, all the intensely widened sub-reaches identified in this work were characterised by low lateral confinement (CI > 8.17; Fig. 7b).

5.3. Implications for geomorphological hazard assessment in flood risk evaluation

Channel widening in mountain rivers can cause dramatic interactions with man-made structures, representing an important hazard source (Stoffel et al., 2016; Surian et al., 2016; Ruiz-Villanueva et al., 2018; Ross et al., 2019). For the 21 sub-reaches characterised by intense channel widening during Vaia, we calculated the expected WR on the basis of statistical models for steep and non-steep channels [Eqs. (3) and (4)], in which WR, ω_{pk}^{pre} and CI were determined at all the sub-reaches investigated in this study. The comparison of the WR expected by statistical models [Eqs. (3) and (4)] and WR observed in response to the Vaia event (Table 5) revealed that at these intensely widened sub-reaches, the WR actually occurring during the flood was in most cases much higher than that predicted by the models. In detail, the observed WR was, on average, 67 % higher than that expected on the basis of Eqs. (3) and (4). The difference between observed and expected WR values reached maximum values of + 131 % at sub-reach L3.1 of the Liera Torrent (Figs. 8c and d) where, compared with an expected WR of 6.9, the observed WR was 15.8, and + 223 % at sub-reach P3.3 of the Pettorina Torrent, where a WR of 10.3 occurred compared with an expected WR of 3.2. Moreover, six of these sub-reaches (Table 5) were characterised by anomalous residuals >2 between the WR predicted by the regression models and the WR actually transpiring during the event.

Our results demonstrate that sub-reaches where intense channel widening arises are associated with likely occurrence of debris flood. It is thus crucial to consider the possible occurrence of debris flood instead of normal water flow at a channel site during a severe hydrological event that can be reasonably determined from a local morphological and sedimentological characterization of a river network (Brenna et al., 2021; Jakob et al., 2022); this allows the reliable prediction of the geomorphic response of a river to a flood. Debris flood can occur in response to high hydrological forcing or take place downstream of debris flow channels delivering large amounts of sediment to a receiving stream. Such conditions may easily transpire during a high-magnitude to extreme hydrological event (as that induced by the Vaia storm at the Pettorina, Liera and Tegnas catchments) at sub-reaches of a mountain river characterised by high slopes (e.g. >4 %–5 %) and narrow sections (<10–15 m) and/or a mountain river located immediately downstream of confluences of steep tributaries prone to debris flow occurrence. Predicting channel widening exclusively using statistical models derived from large data sets that do not distinguish between various transport processes can cause a remarkable underestimation of the channel changes occurring at some sub-reaches possibly affected by debris floods and, therefore, an underestimation of geomorphological hazards.

6. Conclusion

Our results showed that, although statistically significant relationships among width ratio, pre-flood unit stream power and channel confinement were found, under the same controlling factors (CI and ω_{pk}^{pre}) a relatively broad spectrum of WRs was observed along the stream network. In particular, at sub-reaches where intense widening occurred (Fig. 7), channel modifications were much greater than expected by the statistical models constructed in this research (Table 5). All the 21 intensely widened sub-reaches were most likely affected by debris flood during the severe flooding induced by Vaia, with intense channel widening that was associated with certain occurrence of debris floods or highly likely occurrence of debris floods 15 % and 85 % of the times, respectively. These results led us to conclude that the various fluid gravity flows responsible for sediment transport at a mountain river drive various morphological channel responses to a flood. Debris flood is a transport process that often induce channel changes that are considerably more intense than those occurring in response to water flow. However, although debris flood represents a sediment transport process that often promotes intense widening during severe floods, it does not always cause major channel changes and widening.

A limitation affecting our work lies in the reliable but still indirect determination of flow types that occurred during the Vaia storm in the Liera and Pettorina torrents. An improvement toward a better understanding of the control of debris floods on channel widening could be achieved by considering larger datasets of debris floods recognized from field evidence (that was possible in this work only for the Tegnas Torrent), such as the characteristics of flood deposits (e.g. Brenna et al., 2020a), or from the application of more complex holistic approaches that are being developed to determine the likelihood of debris flooding in mountain streams (e.g. Jakob et al., 2022).

Our findings represent a step forward in understanding geomorphic processes in mountain rivers, with specific regard for sediment–water flow types as controlling factors for morphological responses to high-magnitude floods (e.g., floods with recurrence intervals higher than 50–100 years). The findings, in accordance with those of Brenna et al. (2021) and Jakob et al. (2022), suggest that a crucial requirement is to identify, at the local scale, the channel sites of a mountain river that are susceptible to debris flood occurrence in response to a high-magnitude flood because their widening can be remarkably more intense than normally expected. These improvements of knowledge may contribute to better management of the valley floors in mountain regions where, with often limited space for human development, decision on locating man-made structures can have tragic effects especially in the face of increasing frequency of high-magnitude hydrological events (Blöschl et al., 2020).

Declaration of competing interest

The authors declare that they have no known competing financial interests or personal relationships that could have appeared to influence the work reported in this paper.

Data availability

Data will be made available on request.

Acknowledgements

This work was carried out within the RETURN Extended Partnership and received funding from the European Union Next-GenerationEU (National Recovery and Resilience Plan – NRRP, Mission 4, Component 2, Investment 1.3 – D.D. 1243 2/8/2022, PE0000005) and from the University of Padova (research fellowship "Sediment transport during extreme flood events" and DOR funds). Data on lateral connectivity in the Liera catchment were made available by CNR IRPI in the frame of Interreg ITAT3032 SedInOut project. The authors thank Riccardo Boniardi and Gioia Gastaldi for supporting remote sensing data editing. We are grateful to the three anonymous reviewers whose comments improved the quality of the paper.

Appendix A. Supplementary data

Supplementary data to this article can be found online at https://doi.org/10.1016/j.geomorph.2023.108650.

References

Amponsah, W., Marchi, L., Zoccatelli, D., Boni, G., Cavalli, M., Comiti, F., Borga, M., 2016. Hydrometeorological characterization of a flash flood associated with major geomorphic effects: assessment of peak discharge uncertainties and analysis of the runoff response. J. Hydrometeorol. 17 (12), 3063–3077. https://doi.org/10.1175/JHM-D-16-0081.1.

Amponsah, W., Ayral, P.A., Boudevillain, B., Bouvier, C., Braud, I., Brunet, P., Borga, M., 2018. Integrated high-resolution dataset of high-intensity European and Mediterranean flash floods. Earth Syst. Sci. Data 10 (4), 1783–1794. https://doi.org/10.5194/essd-10-1783-2018.

ARPAV, 2019. Livelli e portate medie giornaliere del Torrente Cordevole a Ponte Mas negli anni 2003-18. https://www.arpa.veneto.it/temi-ambientali/idrologia/file-e-allegati/rapporti-e-documenti/idrologia-regionale/idrologia-regionale-la-rete-idrometrica/bacino-del-piave/Relazione_1219_Cordevole_Ponte_Mas_2003-18.pdf.

Bagnold, R.A., 1977. Bed load transport by natural rivers. Water Resour. Res. 13 (2), 303–312. https://doi.org/10.1029/WR013i002p00303.

Bagnold, R.A., 1980. An empirical correlation of bedload transport rates in flumes and natural rivers. Proc. R. Soc. Lond. A 372 (1751), 453–473. https://doi.org/10.1098/rspa.1980.0122.

Baker, V.R., 1994. Geomorphological understanding of floods. In: Geomorphology and Natural Hazards. Elsevier, pp. 139–156. https://doi.org/10.1016/B978-0-444-82012-9.50014-1.

Baker, V.R., Kale, V.S., 1998. The role of extreme floods in shaping bedrock channels. Geophys. Monogr. 107, 153–166.

Baker, V., Kochel, R.C., Patton, P.C., 1988. Flood geomorphology. In: Flood Geomorphology. Wiley-Interscience.

Beeson, C.E., Doyle, P.F., 1995. Comparison of bank erosion at vegetated and non-vegetated channel bends. J. Am. Water Resour. Assoc. 31 (6), 983–990. https://doi.org/10.1111/j.1752-1688.1995.tb03414.x.

Belletti, B., Dufour, S., Piégay, H., 2014. Regional assessment of the multi-decadal changes in braided riverscapes following large floods (Example of 12 reaches in South East of France). Adv. Geosci. 37, 57–71. https://doi.org/10.5194/adgeo-37-57-2014.

Beven, K., Binley, A., 2014. GLUE: 20 years on. Hydrol. Process. 28 (24), 5897–5918. https://doi.org/10.1002/hyp.10082.

Beverage, J.P., Culbertson, J.K., 1964. Hyperconcentrations of suspended sediment. J. Hydraul. Div. 90 (6), 117–128.

Blikra, L.H., Nemec, W., 1998. Postglacial colluvium in western Norway: depositional processes, facies and palaeoclimatic record. Sedimentology 45 (5), 909–960. https://doi.org/10.1046/j.1365-3091.1998.00200.x.

Blöschl, G., Kiss, A., Viglione, A., Barriendos, M., Böhm, O., Brázdil, R., Wetter, O., 2020. Current european flood-rich period exceptional compared with past 500 years. Nature 583 (7817), 560–566. https://doi.org/10.1038/s41586-020-2478-3.

Borga, M., Comiti, F., Ruin, I., Marra, F., 2019. Forensic analysis of flash flood response. Wiley Interdiscip. Rev. Water 6 (2), e1338. https://doi.org/10.1002/wat2.1338.

Braud, I., Borga, M., Gourley, J., Hurlimann, M., Zappa, M., Gallart, F., 2016. Flash floods, hydro-geomorphic response and risk management. J. Hydrol. 541 (Part A), 1–5. https://doi.org/10.1016/j.jhydrol.2016.08.005.

Brenna, A., Surian, N., Ghinassi, M., Marchi, L., 2020a. Sediment–water flows in mountain streams: recognition and classification based on field evidence. Geomorphology 371, 107413. https://doi.org/10.1016/j.geomorph.2020.107413.

Brenna, A., Surian, N., Ghinassi, M., Marchi, L., 2020b. Survey of the vaia storm deposits in the tegnas catchment (Dolomites, Italy): field data and evidence of sediment-water flow types. Data Brief 33, 106415. https://doi.org/10.1016/j.dib.2020.106415.

Brenna, A., Marchi, L., Borga, M., Ghinassi, M., Zaramella, M., Surian, N., 2021. Sediment–water flows in mountain catchments: insights into transport mechanisms as responses to high-magnitude hydrological events. J. Hydrol. 602, 126716 https://doi.org/10.1016/j.jhydrol.2021.126716.

Brierley, G.J., Fryirs, K.A., 2005. Geomorphology and River Management: Applications of the River Styles Framework. John Wiley, Hoboken, NJ.

Buraas, E.M., Renshaw, C.E., Magilligan, F.J., Dade, W.B., 2014. Impact of reach geometry on stream channel sensitivity to extreme floods. Earth Surf. Process. Landf. 39 (13), 1778–1789. https://doi.org/10.1002/esp.3562.

Carling, P.A., 1988. The concept of dominant discharge applied to two gravel-bed streams in relation to channel stability thresholds. Earth Surf. Process. Landf. 13 (4), 355–367. https://doi.org/10.1002/esp.3290130407.

Cavaleri, L., Bajo, M., Barbariol, F., Bastianini, M., Benetazzo, A., Bertotti, L., Umgiesser, G., 2019. The October 29, 2018 storm in Northern Italy–an exceptional event and its modeling. Prog. Oceanogr. 178, 102178 https://doi.org/10.1016/j.pocean.2019.102178.

Cenderelli, D.A., Wohl, E.E., 2003. Flow hydraulics and geomorphic effects of glacial-lake outburst floods in the Mount Everest region, Nepal. Earth Surf. Process. Landf. 28 (4), 385–407. https://doi.org/10.1002/esp.448.

Church, M., Jakob, M., 2020. What is a debris flood? Water Resour. Res. 56 (8) https://doi.org/10.1029/2020WR027144.
Costa, J.E., 1984. Physical geomorphology of debris flows. In: Costa, J.E., Fleisher, P.J. (Eds.), Developments and Applications of Geomorphology. Springer, Berlin, Germany, pp. 268–317. https://doi.org/10.1007/978-3-642-69759-3_9.
Costa, J.E., 1988. Rheologic, geomorphic and sedimentologic differentiation of water floods, hyperconcentrated flows and debris flows. In: Baker, V.R., Kochel, R.C., Patton, P.C. (Eds.), Flood Geomorphology. John Wiley, Hoboken, NJ, pp. 113–122.
Costa, J.E., O'Connor, J.E., 1995. Geomorphically effective floods. Geophys. Monogr. 89, 45- 45.
Coussot, P., Meunier, M., 1996. Recognition, classification and mechanical description of debris flows. Earth Sci. Rev. 40 (3–4), 209–227. https://doi.org/10.1016/0012-8252(95)00065-8.
Da Ros, D., Borga, M., 1997. Use of digital elevation model data for the derivation of the geomorphological instantaneous unit hydrograph. Hydrol. Process. 11 (1), 13–33. https://doi.org/10.1002/(SICI)1099-1085(199701)11:1<13::AID-HYP400>3.0.CO;2-M.
Davolio, S., Della Fera, S., Laviola, S., Miglietta, M.M., Levizzani, V., 2020. Heavy precipitation over Italy from the Mediterranean storm "Vaia" in October 2018: assessing the role of an atmospheric river. Mon. Weather Rev. 148 (9), 3571–3588. https://doi.org/10.1175/MWR-D-20-0021.1.
Dean, D.J., Schmidt, J.C., 2013. The geomorphic effectiveness of a large flood on the Rio Grande in the big Bend region: insights on geomorphic controls and post-flood geomorphic response. Geomorphology 201, 183–198. https://doi.org/10.1016/j.geomorph.2013.06.020.
Ferencevic, M., Ashmore, P., 2012. Creating and evaluating digital elevation model-based stream-power map as a stream assessment tool. River Res. Appl. 28 (9), 1394–1416. https://doi.org/10.1002/rra.1523.
Forzieri, G., Pecchi, M., Girardello, M., Mauri, A., Klaus, M., Nikolov, C., Beck, P.S., 2020. A spatially explicit database of wind disturbances in European forests over the period 2000–2018. Earth Syst. Sci. Data 12 (1), 257–276. https://doi.org/10.5194/essd-12-257-2020.
Giovannini, L., Davolio, S., Zaramella, M., Zardi, D., Borga, M., 2021. Multi-model convection-resolving simulations of the October 2018 Vaia storm over Northeastern Italy. Atmos. Res. 253, 105455 https://doi.org/10.1016/j.atmosres.2021.105455.
Gupta, A., Fox, H., 1974. Effects of high-magnitude floods on channel form: a case study in Maryland Piedmont. Water Resour. Res. 10 (3), 499–509. https://doi.org/10.1029/WR010i003p00499.
Harvey, A.M., 1984. Geomorphological response to an extreme flood: a case from Southeast Spain. Earth Surf. Process. Landf. 9 (3), 267–279. https://doi.org/10.1002/esp.3290090306.
Hauer, C., Habersack, H., 2009. Morphodynamics of a 1000-year flood in the Kamp River, Austria, and impacts on floodplain morphology. Earth Surf. Process. Landf. 34 (5), 654–682. https://doi.org/10.1002/esp.1763.
Hicks, D.M., Gomez, B., 2016. Sediment transport. In: Kondolf, G.M., Piégay, H. (Eds.), Tools in Fluvial Geomorphology. John Wiley & Sons, Hoboken, NJ, pp. 324–356. https://doi.org/10.1002/9781118648551.ch15.
Hooke, J.M., 2015. Variations in flood magnitude–effect relations and the implications for flood risk assessment and river management. Geomorphology 251, 91–107. https://doi.org/10.1016/j.geomorph.2015.05.014.
Hooke, J.M., Mant, J.M., 2000. Geomorphological impacts of a flood event on ephemeral channels in SE Spain. Geomorphology 34 (3–4), 163–180. https://doi.org/10.1016/S0169-555X(00)00005-2.
Hungr, O., Leroueil, S., Picarelli, L., 2014. The Varnes classification of landslide types, an update. Landslides 11 (2), 167–194. https://doi.org/10.1007/s10346-013-0436-y.
Iverson, R.M., 1997. Hydraulic modeling of unsteady debris-flow surges with solid-fluid interactions. In: Chen, C.-L. (Ed.), Proceedings, First International Conference on Debris-Flow Hazards Mitigation: Mechanics, Prediction, and Assessment. Hydraulics Division, American Society of Civil Engineers, New York, NY, pp. 550–560.
Iverson, R.M., 2003. The debris-flow rheology myth. In: Rickenmann, D., Chen, C.-l. (Eds.), Debris-Flow Hazards Mitigation: Mechanics, Prediction, and Assessment. IOS press, Amsterdam, Nederland, pp. 303–314.
Jakob, M., Davidson, S., Bullard, G., Busslinger, M., Collier-Pandya, B., Grover, P., Lau, C.A., 2022. Debris-flood hazard assessments in steep streams. Water Resour. Res. 58 (4), e2021WR030907 https://doi.org/10.1029/2021WR030907.
Jansen, J.D., 2006. Flood magnitude–frequency and lithologic control on bedrock river incision in post-orogenic terrain. Geomorphology 82 (1–2), 39–57. https://doi.org/10.1016/j.geomorph.2005.08.018.
Kale, V.S., 2007. Geomorphic effectiveness of extraordinary floods on three large rivers of the Indian Peninsula. Geomorphology 85 (3–4), 306–316. https://doi.org/10.1016/j.geomorph.2006.03.026.
Kale, V.S., Hire, P.S., 2004. Effectiveness of monsoon floods on the Tapi River, India: role of channel geometry and hydrologic regime. Geomorphology 57 (3–4), 275–291. https://doi.org/10.1016/S0169-555X(03)00107-7.
Krapesch, G., Hauer, C., Habersack, H., 2011. Scale orientated analysis of river width changes due to extreme flood hazards. Nat. Hazards Earth Syst. Sci. 11 (8), 2137–2147. https://doi.org/10.5194/nhess-11-2137-2011, 2011.
Kuhnle, R.A., 2013. Suspended load. In: Shroder, J.F. (Ed.), Treatise on Geomorphology, vol. 9. Elsevier, Amsterdam, Netherlands, pp. 124–136. https://doi.org/10.1016/B978-0-12-374739-6.00234-7.
Langhammer, J., 2010. Analysis of the relationship between the stream regulations and the geomorphologic effects of floods. Nat. Hazards 54 (1), 121–139. https://doi.org/10.1007/s11069-009-9456-2.
Lenzi, M.A., Mao, L., Comiti, F., 2006a. Effective discharge for sediment transport in a mountain river: computational approaches and geomorphic effectiveness. J. Hydrol. 326 (1–4), 257–276. https://doi.org/10.1016/j.jhydrol.2005.10.031.
Lenzi, M.A., Mao, L., Comiti, F., 2006b. When does bedload transport begin in steep boulder-bed streams? Hydrol. Process. 20 (16), 3517–3533. https://doi.org/10.1002/hyp.6168.
Macchi, G., Crema, S., Arziliero, L., Boretto, G., De Fanti, B., Marchi, L., Monegato, G., Cavalli, M., 2022. Assessing debris-flow activity and geomorphic changes caused by an extreme rainstorm: the case study of the Liera catchment (Dolomites, northeastern Italy). Rend. Online Soc. Geol. Ital. 58, 2–8. https://doi.org/10.3301/ROL.2022.13.
Magilligan, F.J., 1992. Thresholds and the spatial variability of flood power during extreme floods. Geomorphology 5 (3–5), 373–390. https://doi.org/10.1016/0169-555X(92)90014-F.
Magilligan, F.J., Phillips, J.D., James, L.A., Gomez, B., 1998. Geomorphic and sedimentological controls on the effectiveness of an extreme flood. J. Geol. 106 (1), 87–96. https://doi.org/10.1086/516009.
Magilligan, F.J., Buraas, E.M., Renshaw, C.E., 2015. The efficacy of stream power and flow duration on geomorphic responses to catastrophic flooding. Geomorphology 228, 175–188. https://doi.org/10.1016/j.geomorph.2014.08.016.
Manville, V., White, J.D.L., 2003. Incipient granular mass flows at the base of sediment-laden floods, and the roles of flow competence and flow capacity in the deposition of stratified bouldery sands. Sediment. Geol. 155 (1–2), 157–173. https://doi.org/10.1016/S0037-0738(02)00294-4.
Mather, A.E., Hartley, A., 2005. Flow events on a hyper-arid alluvial fan: Quebrada Tambores, Salar de Atacama, northern Chile. Geol. Soc. Lond., Spec. Publ. 251 (1), 9–24. https://doi.org/10.1144/GSL.SP.2005.251.01.02.
Molnar, P., Densmore, A.L., McArdell, B.W., Turowski, J.M., Burlando, P., 2010. Analysis of changes in the step-pool morphology and channel profile of a steep mountain stream following a large flood. Geomorphology 124 (1–2), 85–94. https://doi.org/10.1016/j.geomorph.2010.08.014.
Moore, R.J., 2007. The PDM rainfall-runoff model. Hydrol. Earth Syst. Sci. 11 (1), 483–499. https://doi.org/10.5194/hess-11-483-2007.
Motta, R., Ascoli, D., Corona, P., Marchetti, M., Vacchiano, G., 2018. Selvicoltura e schianti da vento: il caso della "tempesta Vaia". In: Foresta. Rivista di Selvicoltura ed Ecologia Forestale, 15, pp. 94–98. https://doi.org/10.3832/efor2990-015.
Mount, N.J., Louis, J., Teeuw, R.M., Zukowskyj, P.M., Stott, T., 2003. Estimation of error in bankfull width comparisons from temporally sequenced raw and corrected aerial photographs. Geomorphology 56 (1–2), 65–77. https://doi.org/10.1016/S0169-555X(03)00046-1.
Nemec, W., 2009. What is a hyperconcentrated flow?. In: 27th IAS Meeting of Sedimentology, Alghero Italy, 20-24.09.2009, Abstract Book, p. 267.
Norbiato, D., Borga, M., Degli Esposti, S., Gaume, E., Anquetin, S., 2008. Flash flood warning based on rainfall thresholds and soil moisture conditions: an assessment for gauged and ungauged basins. J. Hydrol. 362 (3–4), 274–290. https://doi.org/10.1016/j.jhydrol.2008.08.023.
Pellegrini, G., Martini, L., Cavalli, M., Rainato, R., Cazorzi, A., Picco, L., 2021. The morphological response of the Tegnas alpine catchment (Northeast Italy) to a large infrequent disturbance. Sci. Total Environ. 770, 145209 https://doi.org/10.1016/j.scitotenv.2021.145209.
Phillips, J.D., 2002. Geomorphic impacts of flash flooding in a forested headwater basin. J. Hydrol. 269 (3–4), 236–250. https://doi.org/10.1016/S0022-1694(02)00280-9.
Pierson, T.C., Major, J.J., 2014. Hydrogeomorphic effects of explosive volcanic eruptions on drainage basins. Annu. Rev. Earth Planet. Sci. 42, 469–507. https://doi.org/10.1146/annurev-earth-060313-054913.
Pierson, T.C., Costa, J.E., Vancouver, W., 1987. A rheologic classification of subaerial sediment-water flows. In: Debris Flows/Avalanches: Process, Recognition, and Mitigation. Reviews in Engineering Geology, 7. Geological Society of America, pp. 1–12.
Postma, G., 1986. Classification for sediment gravity-flow deposits based on flow conditions during sedimentation. Geology 14 (4), 291–294. https://doi.org/10.1130/0091-7613(1986)14<291:CFSGDB>2.0.CO;2.
Rickenmann, D., 1991. Hyperconcentrated flow and sediment transport at steep slopes. J. Hydraul. Eng. 117 (11), 1419–1439. https://doi.org/10.1061/(ASCE)0733-9429(1991)117:11(1419).
Righini, M., Surian, N., Wohl, E., Marchi, L., Comiti, F., Amponsah, W., Borga, M., 2017. Geomorphic response to an extreme flood in two Mediterranean rivers (northeastern Sardinia, Italy): Analysis of controlling factors. Geomorphology 290, 184–199. https://doi.org/10.1016/j.geomorph.2017.04.014.
Rigon, E., Moretto, J., Rainato, R., Lenzi, M.A., Zorzi, A., 2013. Evaluation of the morphological quality index in the Cordevole river (Bl, Italy). J. Agric. Eng. 44 (3) https://doi.org/10.4081/jae.2013.e15 e15-e15.
Rinaldi, M., Surian, N., Comiti, F., Bussettini, M., 2013. A method for the assessment and analysis of the hydromorphological condition of italian streams: the Morphological Quality Index (MQI). Geomorphology 180, 96–108. https://doi.org/10.1016/j.geomorph.2012.09.009.
Rinaldi, M., Surian, N., Comiti, F., Bussettini, M., 2015. A methodological framework for hydromorphological assessment, analysis and monitoring (IDRAIM) aimed at promoting integrated river management. Geomorphology 251, 122–136. https://doi.org/10.1016/j.geomorph.2015.05.010.
Rinaldi, M., Amponsah, W., Benvenuti, M., Borga, M., Comiti, F., Lucía, A., Surian, N., 2016. An integrated approach for investigating geomorphic response to extreme events: methodological framework and application to the October 2011 flood in the Magra River catchment, Italy. Earth Surf. Process. Landf. 41 (6), 835–846. https://doi.org/10.1002/esp.3902.
Ross, D.S., Wemple, B.C., Willson, L.J., Balling, C.M., Underwood, K.L., Hamshaw, S.D., 2019. Impact of an extreme storm event on river corridor bank erosion and phosphorus mobilization in a mountainous watershed in the northeastern United

States. J. Geophys. Res. Biogeosci. 124 (1), 18–32. https://doi.org/10.1029/2018JG004497.
Ruiz-Villanueva, V., Badoux, A., Rickenmann, D., Böckli, M., Schläfli, S., Steeb, N., Rickli, C., 2018. Impacts of a large flood along a mountain river basin: the importance of channel widening and estimating the large wood budget in the upper Emme River (Switzerland). Earth Surf. Dyn. 6 (4), 1115–1137. https://doi.org/10.5194/esurf-6-1115-2018.
Scorpio, V., Crema, S., Marra, F., Righini, M., Ciccarese, G., Borga, M., Comiti, F., 2018. Basin-scale analysis of the geomorphic effectiveness of flash floods: a study in the northern Apennines (Italy). Sci. Total Environ. 640, 337–351. https://doi.org/10.1016/j.scitotenv.2018.05.252.
Scorpio, V., Cavalli, M., Steger, S., Crema, S., Marra, F., Zaramella, M., Borga, M., Marchi, L., Comiti, F., 2022. Storm characteristics dictate sediment dynamics and geomorphic changes in mountain channels: a case study in the Italian Alps. Geomorphology 108173. https://doi.org/10.1016/j.geomorph.2022.108173.
Sklar, L.S., Riebe, C.S., Genetti, J., Leclere, S., Lukens, C.E., 2020. Downvalley fining of hillslope sediment in an alpine catchment: implications for downstream fining of sediment flux in mountain rivers. Earth Surf. Process. Landf. 45 (8), 1828–1845. https://doi.org/10.1002/esp.4849.
Stoffel, M., Wyżga, B., Marston, R.A., 2016. Floods in mountain environments: a synthesis. Geomorphology 272, 1–9. https://doi.org/10.1016/j.geomorph.2016.07.008.
Surian, N., Righini, M., Lucía, A., Nardi, L., Amponsah, W., Benvenuti, M., Viero, A., 2016. Channel response to extreme floods: insights on controlling factors from six mountain rivers in northern Apennines, Italy. Geomorphology 272, 78–91. https://doi.org/10.1016/j.geomorph.2016.02.002.
Swanson, B.J., Meyer, G.A., Coonrod, J.E., 2011. Historical channel narrowing along the Rio Grande near Albuquerque, New Mexico in response to peak discharge reductions and engineering: magnitude and uncertainty of change from air photo measurements. Earth Surf. Process. Landf. 36 (7), 885–900. https://doi.org/10.1002/esp.2119.
Thompson, C., Croke, J., 2013. Geomorphic effects, flood power, and channel competence of a catastrophic flood in confined and unconfined reaches of the upper Lockyer valley, Southeast Queensland, Australia. Geomorphology 197, 156–169. https://doi.org/10.1016/j.geomorph.2013.05.006.
Waananen, A.O., Harris, D.D., Williams, R.C., 1970. Floods of December 1964 and January 1965 in the Far Western States: Part 2. Streamflow and Sediment Data. Department of the Interior, US Geological Survey, Reston, VA: US.
Wolman, M.G., Miller, J.P., 1960. Magnitude and frequency of forces in geomorphic processes. J. Geol. 68 (1), 54–74. https://doi.org/10.1086/626637.
Yager, E.M., Schott, H.E., 2013. The initiation of sediment motion and formation of armor layers. In: Shroder, J.F. (Ed.), Treatise on Geomorphology, vol. 9. Elsevier, Amsterdam, Netherlands, pp. 87–102.. https://doi.org/10.1016/B978-0-12-374739-6.00232-3.
Yochum, S.E., Sholtes, J.S., Scott, J.A., Bledsoe, B.P., 2017. Stream power framework for predicting geomorphic change: the 2013 Colorado Front Range flood. Geomorphology 292, 178–192. https://doi.org/10.1016/j.geomorph.2017.03.004.
Zaramella, M., Dallan, E., Marchi, L., Marra, F., Cavalli, M., Crema, S., Borga, M., 2023. Characterization of the flood response to the Vaia storm (October 27th-30th, 2018) in a catchment of the Eastern Italian Alps. Submitted to J. Hydrometeorol.
Zaramella, M., Marchi, L., Marra, F., Comiti, F., Crema, S., Marchio, M., Borga, M., 2020. Role of Stationary Convective Bands and Antecedent Conditions on the Flood Response to the Vaia Storm (October 27-30, 2018) in the Eastern Italian Alps, EGU General Assembly 2020, Online, 4–8 May 2020, EGU2020-18668, 2020. https://doi.org/10.5194/egusphere-egu2020-18668.